



Department of
Industry and Resources

**EXPLANATORY
NOTES**

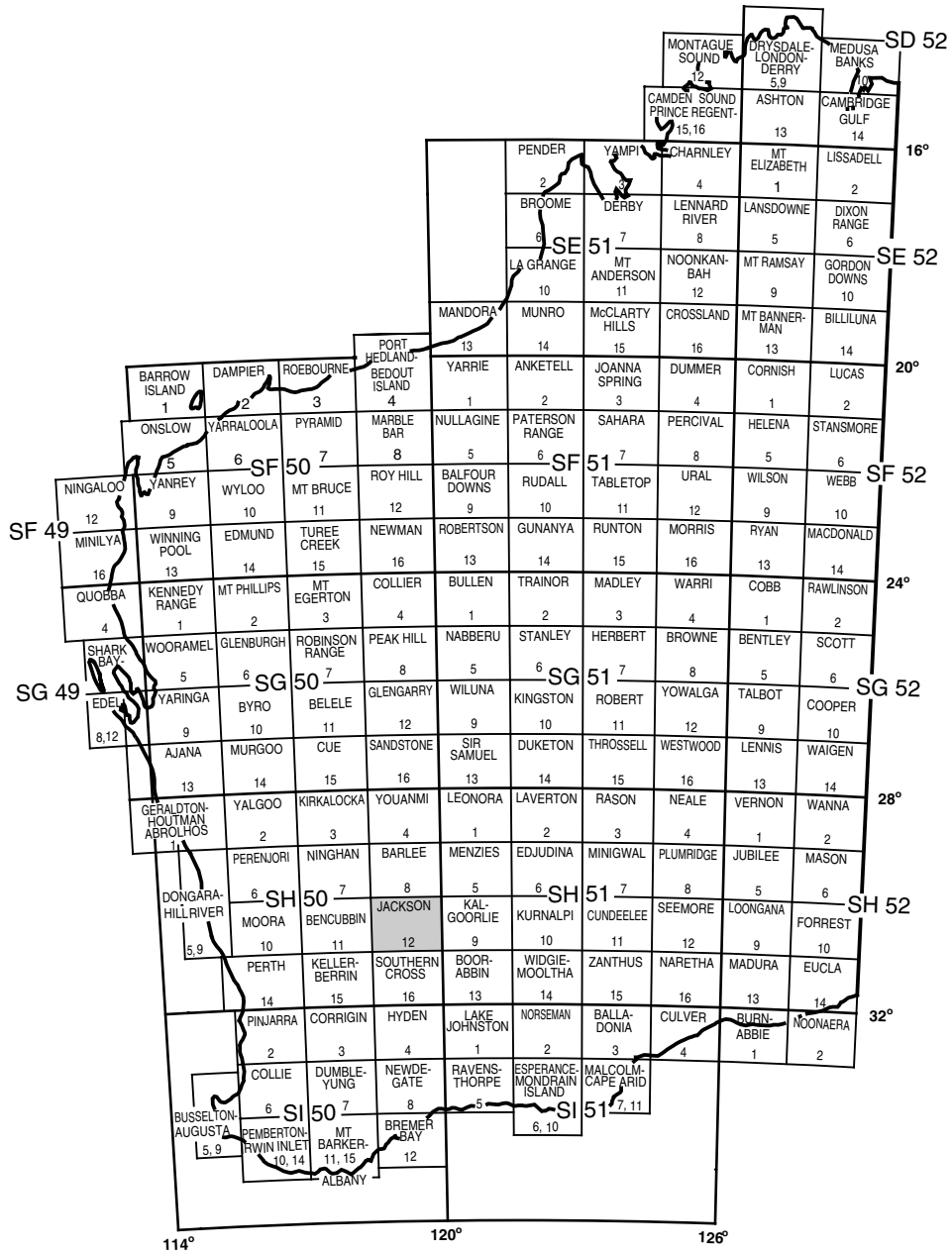
GEOLOGY OF THE BUNGALBIN 1:100 000 SHEET

by **S. F. Chen and S. Wyche**

1:100 000 GEOLOGICAL SERIES



Geological Survey of Western Australia



WOONGARING 2637	JACKSON 2737	BUNGALBIN 2837
JACKSON SH 50-12		
WALYAHMONING 2636	BULLFINCH 2736	SEABROOK 2836

SFC74

17.04.03



GEOLOGICAL SURVEY OF WESTERN AUSTRALIA

**GEOLOGY OF THE
BUNGALBIN
1:100 000 SHEET**

by
S. F. Chen and S. Wyche

Perth 2003

MINISTER FOR STATE DEVELOPMENT
Hon. Clive Brown MLA

DIRECTOR GENERAL, DEPARTMENT OF INDUSTRY AND RESOURCES
Jim Limerick

DIRECTOR, GEOLOGICAL SURVEY OF WESTERN AUSTRALIA
Tim Griffin

REFERENCE

The recommended reference for this publication is:

CHEN, S. F., and WYCHE, S., 2003, Geology of the Bungalbin 1:100 000 sheet: Western Australia Geological Survey, 1:100 000 Geological Series Explanatory Notes, 27p.

National Library of Australia Card Number and ISBN 0 7307 8905 5

ISSN 1321-229X

Grid references in this publication refer to the Geocentric Datum of Australia 1994 (GDA94). Locations mentioned in the text are referenced using Map Grid Australia (MGA) coordinates, Zone 50. All locations are quoted to at least the nearest 100 m.

Copy editor: D. P. Reddy
Cartography: D. Sutton
Desktop publishing: K. S. Noonan
Printed by Haymarket Printing, Perth, Western Australia

Published 2003 by Geological Survey of Western Australia

Copies available from:

Information Centre
Department of Industry and Resources
100 Plain Street
EAST PERTH, WESTERN AUSTRALIA 6004
Telephone: (08) 9222 3459 Facsimile: (08) 9222 3444

This and other publications of the Geological Survey of Western Australia are available online through the Department's bookshop at www.doir.wa.gov.au

Cover photograph:

View to the west from the Yendilberin Hills (MGA 781100E 6633900N); the Taipan gold mine is in the middle distance, and the Helen and Aurora ranges on the horizon.

Contents

Abstract	1
Introduction	1
Location and access	1
Climate, physiography, and vegetation	2
Previous and current investigations	4
Precambrian geology	4
Regional geological setting	4
Archaean rock types	7
Lower greenstone succession	7
Metamorphosed ultramafic rocks (<i>Aup, Aur, Aut, Au, Auk, Aus</i>)	7
Metamorphosed fine-grained mafic rocks (<i>Aba, Abac, Abf, Abm, Abv, Ab, Abg, Abl, Abt</i>)	8
Metamorphosed medium- to coarse-grained mafic rocks (<i>Ao, Aog</i>)	9
Metamorphosed felsic volcanic rocks (<i>Af</i>)	10
Metamorphosed sedimentary rocks (<i>As, Asq, Ass, Ac, Aci</i>)	10
Upper greenstone succession	11
Marda Complex (<i>AfM, AfMr, AfMs, AfMsc, AfMss</i>)	11
Granitoid rocks (<i>Ag, Agf, Agm, Agmf, Agbb, Agb, Agg, Ags</i>)	11
Veins and dykes (<i>q, g</i>)	12
Mafic dykes (<i>Edy</i>)	12
Lithostratigraphy of the Marda–Diemals greenstone belt	13
Lower greenstone succession	13
Upper greenstone succession	14
Structural geology	14
First deformation event (D_1)	16
Second deformation event (D_2)	16
Third deformation event (D_3)	17
Post- D_3 deformation	19
Metamorphism	19
Cainozoic geology	19
Relict units (<i>Rd, Rf, Rfc, Rgp_g, Rk, Rz, Rzu</i>)	19
Depositional units (<i>C, Cgp_g, Clc, Cf, Cq, W, Wf, Wq, A, Ap, L₁, L₂, L_m, S, Sl</i>)	20
Economic geology	20
Gold	20
Iron	21
References	22

Appendices

1. Gazetteer of localities mentioned in the text	25
2. Whole-rock geochemical data for BUNGALBIN	26

Figures

1. Regional geological setting of BUNGALBIN	2
2. Principal localities, tracks, and physiographic features on BUNGALBIN	3
3. Interpreted geological map of the Marda–Diemals greenstone belt and adjacent areas	5
4. Simplified geological map of BUNGALBIN	6
5. First vertical derivative aeromagnetic image of BUNGALBIN	8
6. Interpretive geological map of the Marda–Diemals greenstone belt on BUNGALBIN	13
7. Lithostratigraphic column of the lower greenstone succession on BUNGALBIN	14
8. Simplified geological map of the Marda Complex	15
9. Lithostratigraphic column of the Marda Complex	16
10. AFM plot indicating the calc-alkaline affinity of the Marda Complex volcanic rocks	16
11. Gently plunging mineral lineation in the Mount Dimer Shear Zone	18
12. S–C fabrics in strongly foliated monzogranite, showing a sinistral shear sense in the Mount Dimer Shear Zone	18

Table

1. Geological evolution of BUNGALBIN and adjacent areas	17
---	----

Geology of the Bungalbin 1:100 000 sheet

by

S. F. Chen and S. Wyche

Abstract

The BUNGALBIN 1:100 000 sheet is situated in the central Southern Cross Granite–Greenstone Terrane of the Yilgarn Craton. It covers the southeastern part of the Marda–Diemals greenstone belt, the northern part of the Hunt Range greenstone belt, the southern end of the Mount Manning greenstone belt, and a small part of the Yerilgee greenstone belt. These greenstone belts are separated by large areas of granitoid rocks of mainly monzogranitic composition.

On BUNGALBIN the Marda–Diemals greenstone belt consists of a 3 Ga mafic-dominated lower greenstone succession that is subdivided into three lithostratigraphic associations. The lower association is dominated by tholeiitic basalt, with subordinate ultramafic rocks in its lower part, and thin units of banded iron-formation and chert in its upper part. The middle association is composed of a major banded iron-formation and chert unit, up to 800 m thick, with intercalated lenticular quartzites. The upper association comprises a variety of rock types, including tholeiitic and high-Mg basalts, a number of banded iron-formation and chert units, and minor siltstone and shale. The lower greenstone succession is unconformably overlain by a c. 2.73 Ga upper greenstone succession that consists of felsic volcanic and volcanoclastic sedimentary rocks of the Marda Complex. In other greenstone belts on BUNGALBIN, only the lower greenstone succession is recognized.

Emplacement of the Butcher Bird Monzogranite was coeval with deposition of the Marda Complex. However, most granitoid rocks are younger than the greenstones. Granitoid rocks are variably deformed, with high strain partitioned into the northwesterly trending Mount Dimer Shear Zone and some granite–greenstone contacts.

Three principal deformation events have been recognized on BUNGALBIN. D₁ north–south compression produced low-angle thrust faults, bedding-parallel foliation, and tight to isoclinal folds in the lower greenstone succession. D₂ east–west compression represents a regional folding event that produced macroscopic folds with a weakly developed axial-planar foliation in greenstones, and a north-trending foliation in high-strain zones within granitoid rocks. D₃ progressive and inhomogeneous, east–west shortening developed the northwest-trending, sinistral Mount Dimer Shear Zone, and reoriented the F₂ Bungalbin Syncline into its current northwest trend. Post-D₃ deformation produced northeast- and east-trending fractures and faults, some of which are filled by quartz veins and Proterozoic mafic dykes. All Archaean greenstones and granitoid rocks have been metamorphosed. The metamorphic grade is typically low to moderate, with some rocks of middle-amphibolite facies.

Gold has been produced from a number of sites, of which the Mount Dimer gold mine is the most significant. Iron-ore deposits have been identified in the Bungalbin Hill area.

KEYWORDS: Archaean, granite–greenstone belt, Marda–Diemals, Southern Cross Granite–Greenstone Terrane, Yilgarn Craton, gold, iron ore.

Introduction

Location and access

The BUNGALBIN* 1:100 000 geological map sheet (SH 50-12, 2837) lies in the northeastern part of the JACKSON 1:250 000 sheet (Fig. 1) and is bounded by latitudes 30°00' and 30°30'S and longitudes 119°30' and 120°00'E. The name of the map sheet is derived from Bungalbin Hill†, which forms part of the Helena and Aurora ranges (Fig. 2), rising to 684 m above the Australian Height Datum (AHD).

Access to BUNGALBIN is provided by the Menzies–Evanston Road from Kalgoorlie and by the Bullfinch–Evanston Road from Perth. About 160 km west of Menzies, these two roads intersect. Following the Bullfinch–Evanston Road 62 km from the intersection to the south, the road meets a major track, near the abandoned Marda Dam, leading to BUNGALBIN. This track is approximately 102 km north of Bullfinch, 135 km north of Southern Cross, and 29 km west of the western

* Capitalized names refer to standard 1:100 000 map sheets, unless otherwise indicated.

† MGA coordinates of localities mentioned in the text are listed in Appendix 1.

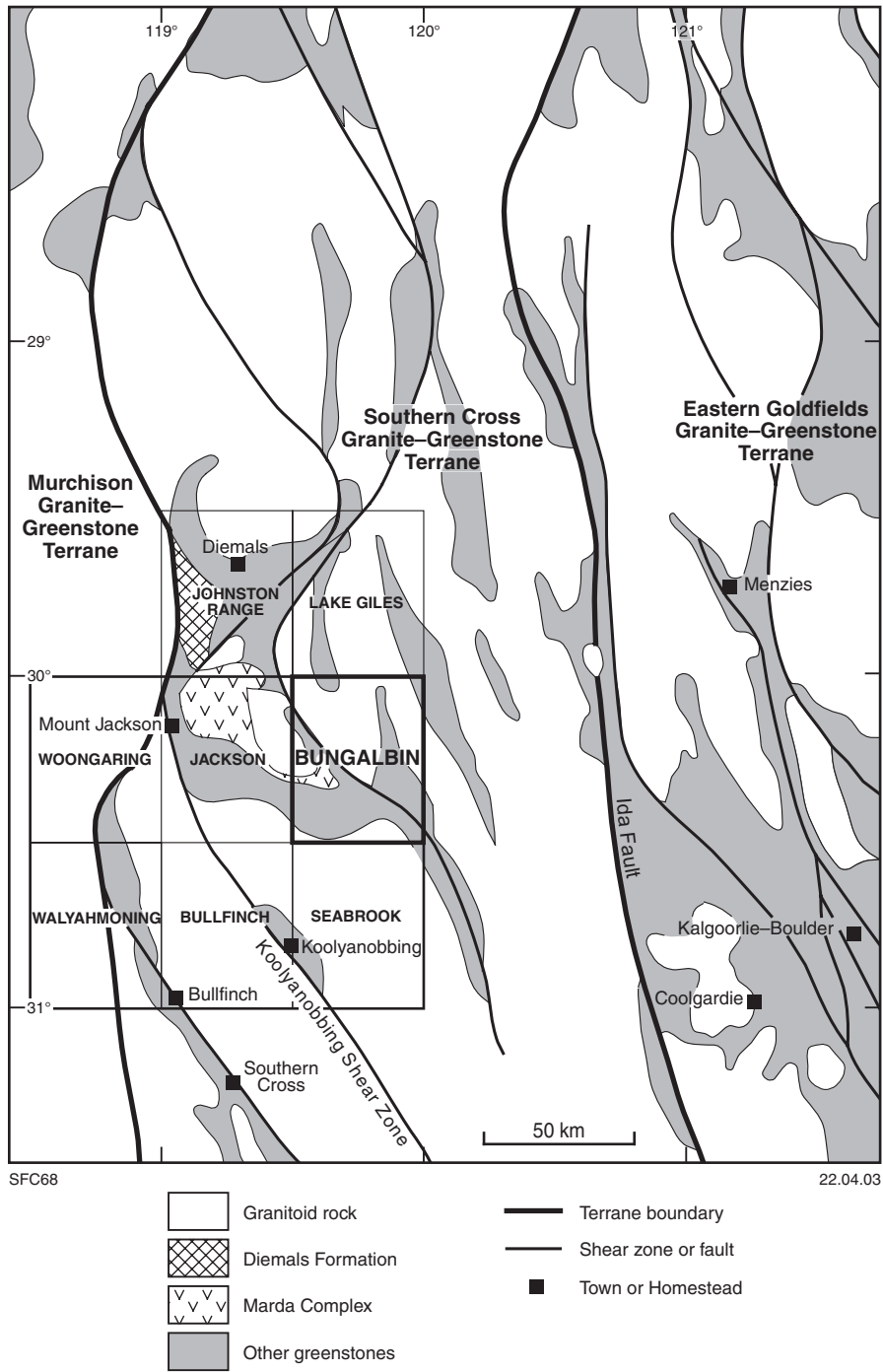


Figure 1. Regional geological setting of BUNGALBIN

boundary of BUNGALBIN. In addition, roads associated with gold mining activity and iron ore exploration within BUNGALBIN link the Aurora and Mount Dimer mine sites (Fig. 2) with Koolyanobbing and the Great Eastern Highway respectively.

There are no permanent residents in the BUNGALBIN sheet area, although temporary camps have been established at the Aurora and Mount Dimer mine sites. Most of the greenstones within BUNGALBIN are accessible via tracks and exploration grids, whereas access to granitoid rocks is generally difficult.

Climate, physiography, and vegetation

The climate of BUNGALBIN is semi-arid. Average annual rainfall is similar to the Diemals Homestead (276 mm)* to the northwest, and Southern Cross (286 mm) to the south. Rain falls mainly in winter, with occasional major summer rainfall events due to tropical influences from the

* Climate data for Diemals Homestead and Southern Cross are from the Commonwealth Bureau of Meteorology website, 2002.

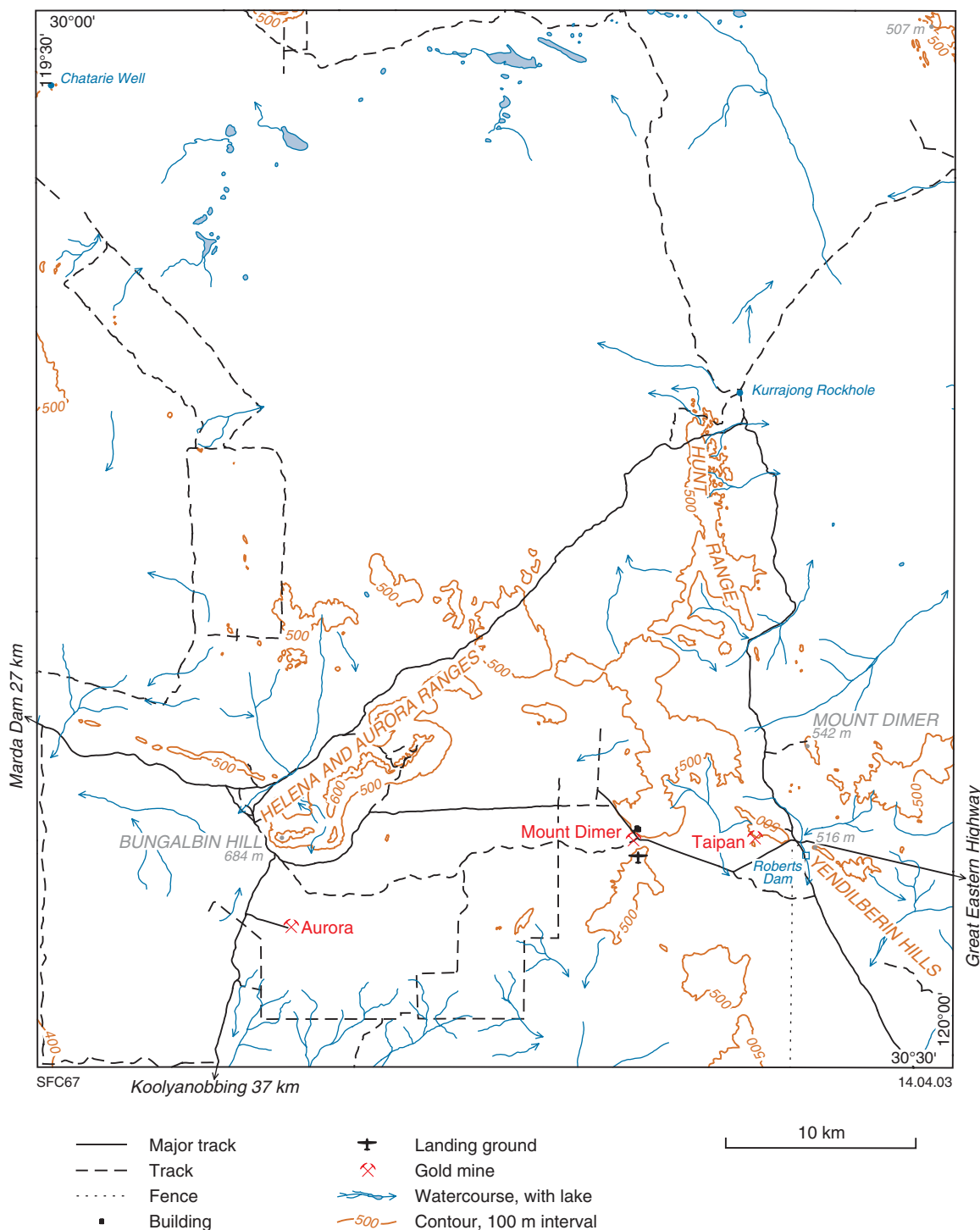


Figure 2. Principal localities, tracks, and physiographic features on BUNGALBIN

north. During the summer months the climate is hot and dry, with maximum temperatures generally higher than 30°C between November and March. Winter is cold, with occasional frosts from June to August.

The physiography of BUNGALBIN is shown in Figure 2. The most prominent topographic feature is the Helena and Aurora ranges in the southwest, where a major banded iron-formation and chert unit forms ridges up to 704 m

above AHD, about 200 m higher than the surrounding areas. The Hunt Range and Yendilberin Hills in the east have elevations up to 550 m, corresponding to banded iron-formation and chert ridges. In other areas, elevations range from 400 to 500 m.

On BUNGALBIN, small playa lakes near the northern edge of the sheet area (Fig. 2) form part of the Lake Giles system. Other major playa lake systems around BUNGALBIN

include the Hamersley Lakes to the west, and the Lake Deborah – Lake Seabrook – Lake Walton system to the south. The present-day drainage on BUNGALBIN is mainly controlled by the distribution of these playa lake systems.

BUNGALBIN lies entirely within the Coolgardie Botanical District or Southwestern Interzone of Beard (1990). The region is characterized by eucalypt woodlands and open woodlands dominated by *Eucalyptus salmonophloia*, *E. salubris*, and *E. loxophleba*, with patches of *Acacia* scrub and mallee, and a typical understorey of saltbush or broombush with sparse perennial and annual grasses. Vegetation on banded iron-formation and chert ridges is low (1.5 – 2.5 m), with dense thickets of *Acacia* and *Casuarina* species. Sandplains over granitoid rocks are dominated by *Acacia* thickets, interspersed with small, low woodland patches, with locally developed hummocky spinifex grass. Detailed descriptions of the ecosystems on BUNGALBIN are given by Beard (1979, 1990) and the Biological Surveys Committee (1985).

Previous and current investigations

Driven by gold mining activity in the region, Woodward (1912) and Blatchford and Honman (1917) produced geological sketch maps with preliminary descriptions that cover most of the JACKSON and BARLEE 1:250 000 sheets. On these geological sketch maps, greenstones were separated from granitoid rocks, but both greenstones and granitoid rocks were not further subdivided. The geology and gold production of mining centres between Southern Cross and Diemals were summarized by Matheson and Miles (1947). The results of an airborne magnetic and radiometric survey in 1957 were reported by Spence (1958). Based on these results, the Bureau of Mineral Resources (1965) published four maps that covered the JACKSON 1:250 000 sheet and clearly delineated the dominant structural trends. The first systematic geological mapping in the region is represented by the JACKSON 1:250 000 geological map (Chin and Smith, 1983). Based on this map and newly acquired aeromagnetic data (Geoscience Australia, 1997, Project 696), an interpreted geological map was produced by Mackey (1999).

Other relevant studies concerning the central Yilgarn Craton include Bye (1968), Hallberg et al. (1976), and Taylor and Hallberg (1977), who investigated the geochemical and volcanological characteristics of felsic to intermediate volcanic rocks in the Marda Complex. Ahmat (1986) described the metamorphic grade variations in the Southern Cross Granite–Greenstone Terrane. Griffin (1990) summarized the geology of granite–greenstones for the whole terrane in a review based on the published 1:250 000-scale geological maps. Dalstra (1995) and Dalstra et al. (1998, 1999) conducted a regional metamorphic, structural, and mineralization study between Southern Cross and Diemals.

Extensive exploration for gold and iron ore has been carried out in the region since the 1970s. Company reports, including unpublished maps and exploration data, are

available through the Western Australia mineral exploration (WAMEX) open-file database system at the Department of Industry and Resources (formerly Department of Mineral and Petroleum Resources) in Perth and at the Kalgoorlie Regional Office of the Geological Survey of Western Australia (GSWA).

This 1:100 000-scale geological mapping on BUNGALBIN by the GSWA was undertaken in 1998–99 using 1:25 000-scale colour aerial photographs taken in October 1997 by the Western Australian Department of Land Administration (DOLA). Map compilation was assisted by Landsat Thematic Mapper (TM5) imagery processed by DOLA, and aeromagnetic images derived from the newly acquired 400 m line-spaced dataset (Geoscience Australia, 1997, Project 696). Interpretation of the bedrock geology was also aided by exploration drillhole data collected during the course of field mapping.

Precambrian geology

Regional geological setting

BUNGALBIN is in the central part of the Southern Cross Granite–Greenstone Terrane of the Yilgarn Craton (Fig. 1). The Archaean Yilgarn Craton is subdivided into the Narryer and South West Terranes, which are dominated by granite and granitoid gneiss, and the Murchison, Southern Cross, and Eastern Goldfields Granite–Greenstone Terranes (Tyler and Hocking, 2001). These terranes broadly correspond to the provinces of Gee et al. (1981) and the superterrane of Myers (1997). Recent geological and geochronological data suggest that the Southern Cross Granite–Greenstone Terrane shares some common aspects of lithostratigraphy, greenstone geochronology, and tectonic history with the Murchison Granite–Greenstone Terrane, but has much older greenstones and deformation events than the Eastern Goldfields Granite–Greenstone Terrane (Chen et al., in press; cf. Barley and Groves, 1990; Watkins and Hickman, 1990; Pidgeon and Hallberg, 2000; Greenfield et al., 2000).

BUNGALBIN covers the southeastern part of the Marda–Diemals greenstone belt (Figs 3 and 4), which comprises two greenstone successions. A 3 Ga lower greenstone succession is characterized by mafic volcanic rocks and banded iron-formation and has been subdivided into three lithostratigraphic associations: lower, middle, and upper (Chen and Wyche, 2001b; Wyche et al., 2001a; Riganti and Chen, 2002; Chen et al., in press). The lower association consists mainly of tholeiitic basalt with subordinate ultramafic rock and high-Mg basalt; the middle association is characterized by banded iron-formation and chert; and the upper association contains a variety of rock types but is dominated by mafic volcanic rocks (Chen and Wyche, 2001b; Chen et al., in press). The lower greenstone succession is unconformably overlain by a 2.73 Ga upper greenstone succession that consists of felsic to intermediate volcanic rocks (Marda Complex; Hallberg et al., 1976; Chin and Smith, 1983; Riganti and Chen, 2002), and clastic sedimentary rocks (Diemals Formation; Walker and Blight, 1983; Wyche et al., 2001a).

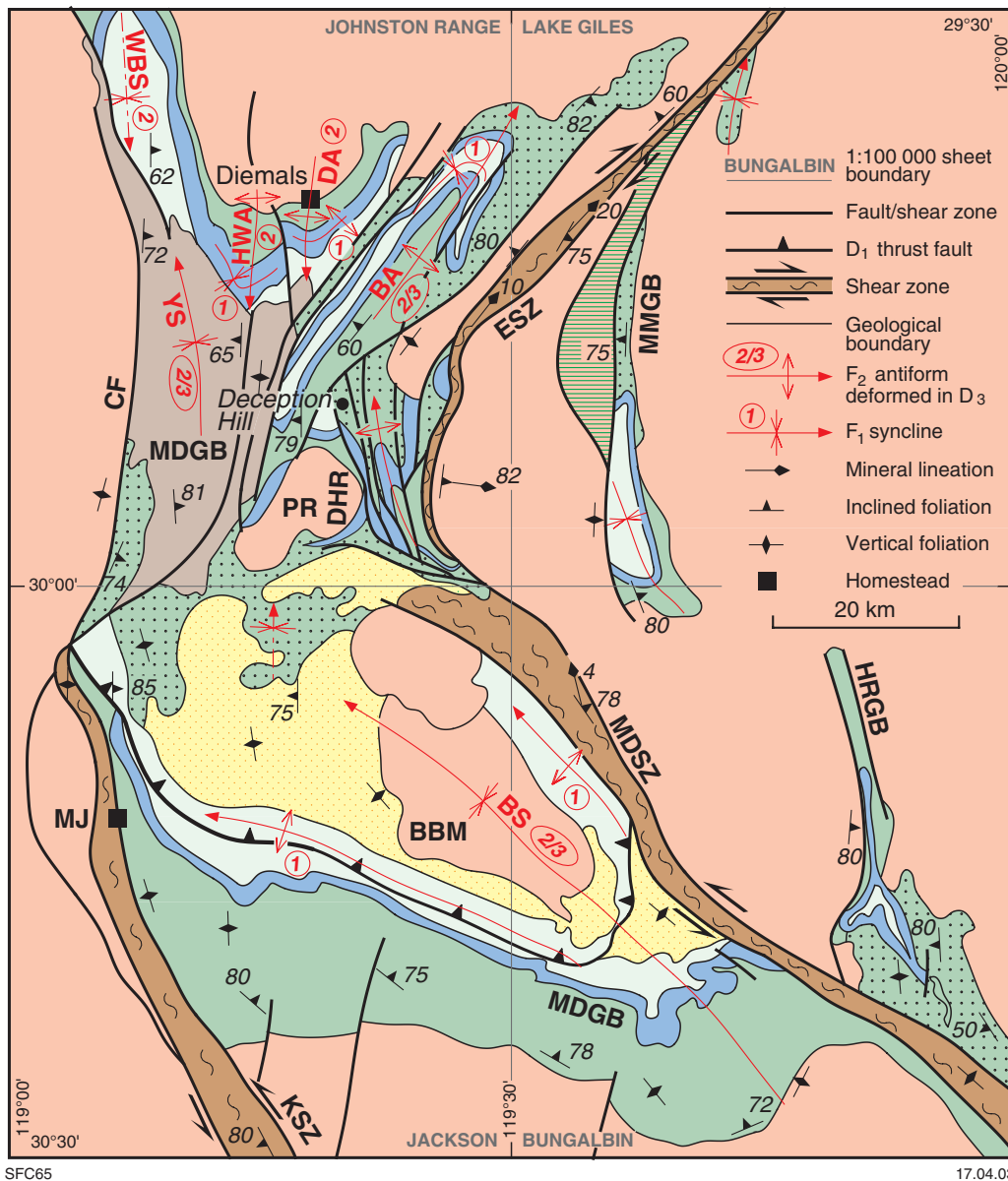
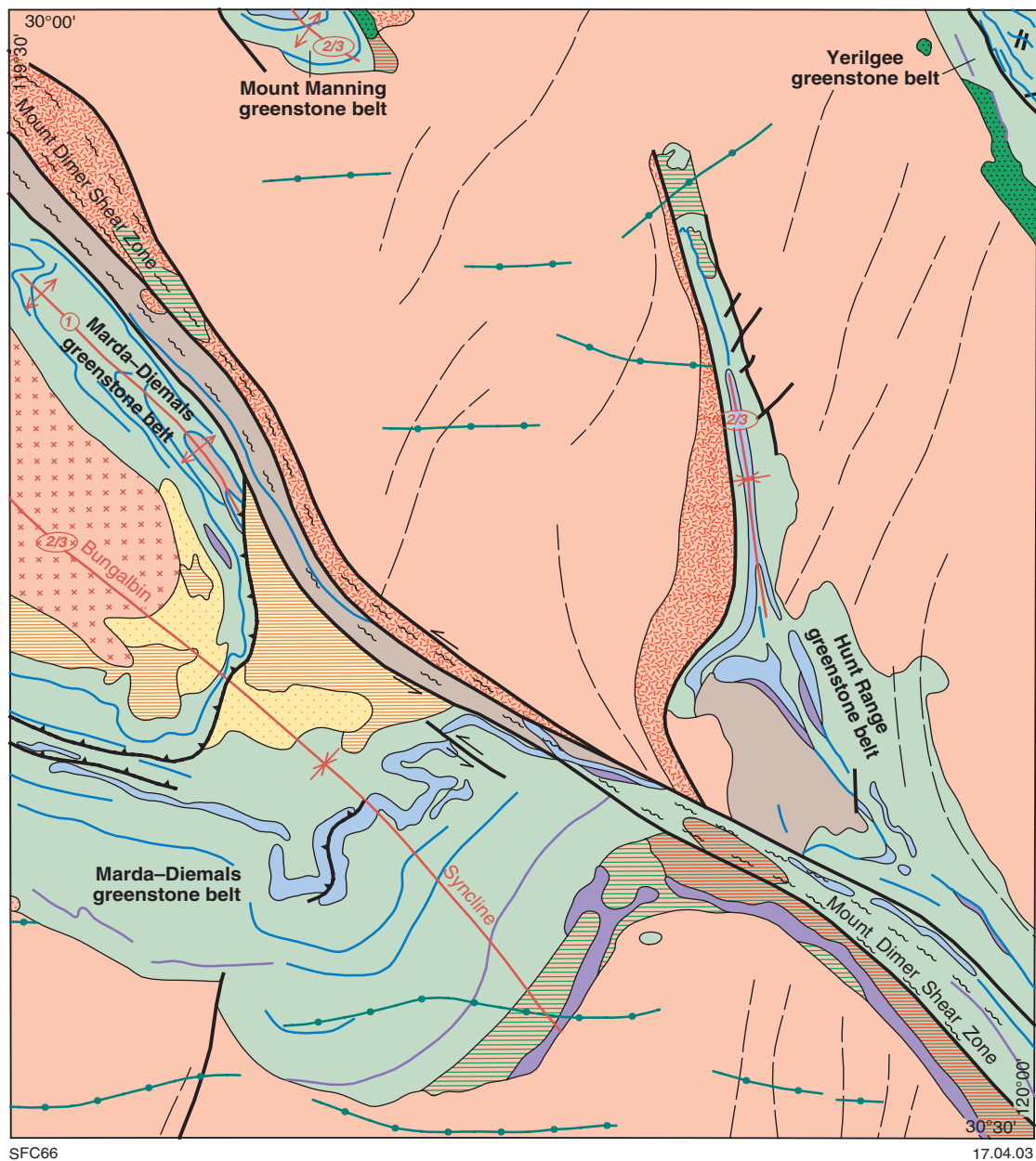


Figure 3. Interpreted geological map of the Marda-Diemals greenstone belt and adjacent areas, showing the distribution of the lower and upper greenstone successions and structural elements. Shear zones: ESZ = Evanston, KSZ = Koolyanobbing, MDSZ = Mount Dimer. Folds: BA = Broadbents Antiform, BS = Bungalbin Syncline, DA = Diemals Anticline, HWA = Horse Well Anticline, WBS = Watch Bore Syncline, YS = Yarbu Syncline. Greenstone belts: HRGB = Hunt Range, MDGB = Marda-Diemals, MMGB = Mount Manning. BBM = Butcher Bird Monzogranite, CF = Clampton Fault, DHR = Die Hardy Range, MJ = Mount Jackson Homestead, PR = Pigeon Rocks Monzogranite (after Chen et al., in press; Chen and Wyche, 2001a; Greensfield, 2001; Riganti and Chen, 2000; Wyche et al., 2000)



SFC66

17.04.03

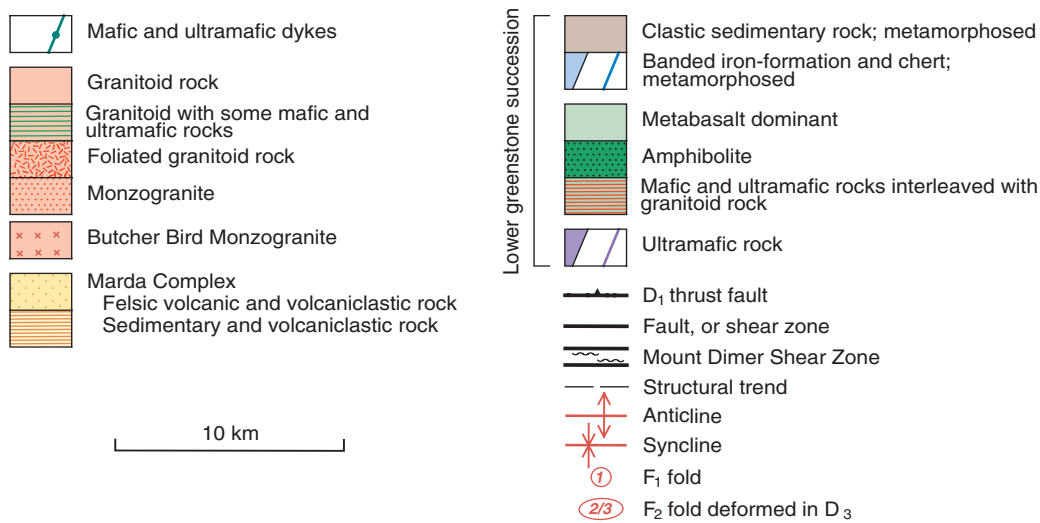


Figure 4. Simplified geological map of BUNGALBIN

Along with the Marda–Diemals greenstone belt, parts of the Hunt Range, Mount Manning, and Yerilgee greenstone belts (Griffin, 1990; Greenfield, 2001) are also exposed in the BUNGALBIN sheet area (Fig. 4). The northern part of the Hunt Range greenstone belt is locally well exposed and contains rocks that may correlate with the lower two associations of the lower greenstone succession in the Marda–Diemals greenstone belt. In this area the lower association comprises basalt with interleaved lenticular high-Mg basalt and gabbro, and the middle association consists of a prominent unit of chert and banded iron-formation with a discontinuous quartzite at the base. The southern part of the Hunt Range greenstone belt is poorly exposed in the Mount Dimer and Yendilberin Hills areas, where it contains basalt, banded iron-formation, clastic sedimentary rocks, and subordinate ultramafic rocks.

Most of the Mount Manning greenstone belt lies on LAKE GILES (Greenfield, 2001), but its southern end is exposed in the northern part of BUNGALBIN (Figs 3 and 4). Here, the possible correlative of the Marda–Diemals lower association comprises amphibolite and basalt interleaved with thin units of banded iron-formation, chert, and gabbro, whereas a prominent ridge-forming chert and banded iron-formation unit may correlate with the middle association of the Marda–Diemals greenstone belt.

The northern part of the Yerilgee greenstone belt on LAKE GILES consists of banded iron-formation, chert, high-Mg basalt, ultramafic rock, gabbro, basalt, and clastic sedimentary rocks. However, the greenstone lithostratigraphy has not been established due to poor exposure and structural complexity (Greenfield, 2001). A small part of the Yerilgee greenstone belt in the northeastern corner of BUNGALBIN (Fig. 4) contains rocks that may be equivalent to the lower and middle associations of the Marda–Diemals succession. The structurally, and probably stratigraphically, lowest rocks in the succession are dominated by mafic rocks, with at least two major units of ultramafic rocks. Extensive cover of ferruginous duricrust in the northeastern corner of the sheet area largely conceals a suite of rocks containing abundant banded iron-formation and chert with intercalated mafic intrusive and extrusive rocks that appear to include substantial amounts of high-Mg basalt.

Three principal deformation events have been recognized in the Marda–Diemals and adjacent areas (Chen et al., 2001; Chen and Wyche, 2001b; Greenfield, 2001; Wyche et al., 2001a,b; Riganti and Chen, 2002; Chen et al., in press). D₁ north–south compression produced low-angle thrusts, a gently dipping foliation, and tight to isoclinal folds (Greenfield and Chen, 1999; Chen and Wyche, 2001b). D₂ east–west orogenic compression produced originally northerly trending macroscopic upright folds with a weak axial-planar foliation. D₃ progressive, inhomogeneous east–west shortening produced regional-scale, northwest-trending, sinistral shear zones and northeast-trending dextral shear zones forming arcuate structures (Chen et al., 2001).

Two styles of metamorphism have been recognized in the central Yilgarn Craton: early, very low grade metamorphism possibly related to sea-floor alteration; and later

low- to medium-grade metamorphism that coincided with a period of widespread granitoid intrusion (Ahmat, 1986; Dalstra, 1995; Dalstra et al., 1999).

Archaean rock types

All Archaean rocks on BUNGALBIN have been metamorphosed, but primary textures are commonly preserved and protoliths can be inferred in most cases. For ease of description, the prefix ‘meta’ may be omitted and protolith rock names used in the following descriptions.

Lower greenstone succession

Metamorphosed ultramafic rocks (*Aup*, *Aur*, *Aut*, *Au*, *Auk*, *Aus*)

Ultramafic rocks constitute only a small proportion of greenstones on BUNGALBIN. Aeromagnetic images show a major ultramafic unit at the preserved base of the Marda–Diemals greenstone belt in the southeast (Figs 4 and 5). It is poorly exposed as peridotite (*Aup*; MGA 785500E 6622300N), and silica caprock (*Rzu*) at a number of places (e.g. MGA 765700E 6627600N; see **Cainozoic geology**). Exploration drillhole data reveal that there are also tremolite–chlorite(–tal) schist (*Aur*) and talc–chlorite schist (*Aut*) within this ultramafic unit. Elsewhere, scattered outcrops of ultramafic rock (*Aup*, *Aur*) are mainly concentrated in the lower part of the greenstone stratigraphy.

Undivided metamorphosed ultramafic rocks (*Au*) are typically deeply weathered and consist of brown and pale-green, schistose, chlorite-rich rocks that are commonly associated with silica caprock (*Rzu*). A metakomatiite (*Auk*) unit, about 100 m thick, is well exposed in the northeastern limb of the Bungalbin Syncline (MGA 750600E 6651400N and 750200E 6652250N). The komatiite contains both random and platy olivine-spinifex textures (Donaldson, 1982), with pseudomorphed olivine plates up to 5 cm long. The komatiite is intercalated with and overlain by high-Mg basalts that have typical pyroxene-spinifex textures. A small outcrop of komatiite on the western side of the Yerilgee greenstone belt (MGA 788100E 6671900N) is strongly chloritized, but preserves medium-grained, olivine-spinifex texture.

Small bodies of peridotite (*Aup*) are typically low in the greenstone succession, commonly near the granite–greenstone contacts. Massive to weakly deformed peridotite may intrude mafic volcanic rocks as there is commonly no clear association with komatiite. However, peridotite and silica caprock with relict cumulate textures are exposed near the komatiite outcrop on the western side of the Yerilgee greenstone belt. The peridotite is composed of medium- to coarse-grained olivine with interstitial pyroxene. The rocks are typically metamorphosed, with olivine pseudomorphed by serpentine and chlorite. These rocks commonly contain abundant accessory magnetite. Although peridotite is typically serpentized, cumulate textures may be preserved by fine magnetite outlining original olivine grains (e.g. MGA 742500E 6634600N). Analyses of two peridotites are presented in Appendix 2 (GSWA 159442 and 143363).



Figure 5. First vertical derivative aeromagnetic image of BUNGALBIN (based on 400m line-spaced data)

Tremolite–chlorite(–talc) schist (*Aur*) is exposed in discontinuous lenses in strongly deformed mafic volcanic rocks adjacent to granite–greenstone contacts, low in the greenstone lithostratigraphy. The preferred alignment of fine- to coarse-grained tremolite and chlorite defines a pervasive foliation. Tremolite–chlorite(–talc) schist (*Aur*) and subordinate talc–chlorite schist (*Aut*) are easily weathered and fresh material is commonly only in mineral exploration drillholes in areas such as the Mount Dimer Shear Zone in southeastern BUNGALBIN. These rocks are greenish-grey when fresh, and become light brown after weathering. The majority of tremolite–chlorite(–talc) schists are probably derived from ultramafic rocks, although their protoliths cannot be readily identified. Some

tremolite–chlorite(–talc) schist contains minor feldspar and may have been derived from high-Mg basalt. Serpentinite (*Aus*), which is found in mineral exploration drillholes near the Mount Dimer gold mine, consists dominantly of serpentine with lesser amounts of talc, chlorite, and magnetite. No relic igneous textures are preserved in these rocks.

Metamorphosed fine-grained mafic rocks (*Aba, Abac, Abf, Abm, Abv, Ab, Abg, Abi, Abt*)

Fine-grained mafic rocks are widely distributed on BUNGALBIN. Amphibolite (*Aba, Abac*) and strongly foliated basalt (*Abf*) lie on or adjacent to granite–greenstone

contacts. High-Mg basalt (*Abm*) is mainly distributed in the northeastern limb of the Bungalbin Syncline, in the upper part of the lower greenstone succession, but may also be quite abundant in the poorly exposed Yerilgee greenstone belt. Massive to weakly deformed basalt (*Abv*) is the dominant component of the lower greenstone succession. Other fine-grained mafic rocks (*Ab*, *Abg*, *Abl*, *Abt*) are preserved locally on BUNGALBIN.

Undivided fine-grained mafic rocks (*Ab*) are typically deeply weathered and may be lateritized. They are massive to weakly deformed and range in colour from yellowish-brown to dark purplish to reddish-brown, without distinctive mineralogical or textural features. They are classified as mafic rocks mainly because of the absence of primary quartz and their association with fresh basalt in outcrops and drillholes.

Amphibolite (*Aba*) on BUNGALBIN is mainly exposed on the eastern side of the Mount Manning greenstone belt and the western side of the Yerilgee greenstone belt. In outcrop amphibolite is typically a very dark grey-green to black, fine- to medium- grained, strongly recrystallized, mafic rock. It has a steep pervasive foliation defined by segregation and alignment of mafic minerals and plagioclase. A steeply plunging to down-dip mineral lineation is locally observed on foliation surfaces (e.g. MGA 757800E 6677800N). In thin section plagioclase is recrystallized and commonly untwinned, and hornblende is olive-green to dark blue-green and strongly pleochroic. Amphibolite with calc-silicate minerals (*Abac*) has been mapped in the northeastern corner of BUNGALBIN, on the western side of the Yerilgee greenstone belt (MGA 788000E 6670400N). The rock is typically very fine grained, and characterized by alternating light and dark bands ranging from 0.2 to 1.5 mm in width. The dark bands contain light to dark green, strongly pleochroic amphibole, and the light bands are dominated by fine diopside. Untwinned plagioclase is abundant in the dark layers, but rare in the leucocratic layers. Epidote is a common secondary constituent.

Strongly foliated to amphibolitic basalt (*Abf*) is mainly distributed along the southwestern and southeastern margins of the Marda–Diemals greenstone belt on BUNGALBIN (e.g. MGA 752700E 6626600N, and 741400E 6634400N). It is intercalated with lenticular gabbro and tremolite–chlorite schist, and has a gradational boundary with massive to weakly deformed basalt away from the greenstone margins. Recrystallization is typically weak in foliated basalt, but is relatively strong in more amphibolitic basalt. A well-developed, steep foliation in these rocks is parallel to the granite–greenstone contacts, and may contain a locally preserved, steeply plunging mineral lineation.

Where mafic rocks and minor granitoid rocks are irregularly interleaved and cannot be separated at 1:100 000 scale, they are mapped together as *Abg* (e.g. basalt and gabbro are patchily intruded by medium- to coarse-grained monzogranite around MGA 758700E 6676000N). Pyroxene-spinifex-textured high-Mg basalt is patchily intruded by medium-grained monzogranite in the eastern part of the Hunt Range greenstone belt (around MGA 782100E 6644800N). In these cases both the

monzogranite and mafic rocks are massive to weakly deformed. Within and adjacent to the southeastern section of the Mount Dimer Shear Zone (Fig. 4), exploration drillhole data indicate that basalt, gabbro, and ultramafic schist are interleaved with granitoid rocks.

Chlorite schist (*Abl*) is typically fine, brown, weathered schist that is not clearly derived from ultramafic rock. It is commonly identified in mineral exploration drillholes.

High-Mg basalt (*Abm*) is readily recognized by the relict pyroxene-spinifex texture or variolitic texture (or both). The spinifex (e.g. MGA 750400E 6651400N) is characterized by randomly oriented tremolite–actinolite crystals that have replaced acicular clinopyroxene, ranging in length from a few millimetres up to more than 1 cm, in a fine-grained groundmass of tremolite, actinolite, chlorite, and plagioclase. Varioles, ranging from 5 to 15 mm in size, are present locally. The pyroxene-spinifex-textured high-Mg basalt locally contains prominent pillow structures (e.g. MGA 741200E 6664800N). Pillows range from 30 to 100 cm in size and indicate a younging direction towards the southwest.

The thickness of grey to pale-grey mafic tuff (*Abt*) varies from a few metres up to 50 m (e.g. MGA 741500E 6644200N). It is thinly bedded and laminated, with individual beds ranging from less than 1 mm up to 3 cm in thickness. Although most mafic tuff outcrops are rubbly, in situ bedding is preserved locally (e.g. MGA 775800E 6657100N). In thin section the tuffaceous rocks are very fine grained and consist of cryptocrystalline chlorite, amphibole, and plagioclase, with minor quartz and opaque minerals. The well-bedded mafic tuff is commonly intercalated with massive basaltic flows.

Massive to weakly deformed metabasalt (*Abv*) is the dominant mafic rock type in all greenstone belts on BUNGALBIN. It is typically a grey, fine- to very fine grained rock consisting of light- to dark-green, commonly pleochroic amphibole, plagioclase, and minor quartz and opaque minerals. Secondary epidote and chlorite may also be present. Primary igneous textures, such as spherical and elliptical amygdales filled by quartz and chlorite, have been locally observed. Most metabasalt has probably undergone low-grade (greenschist-facies) metamorphism. However, metamorphic grades are higher, locally up to amphibolite facies, near granite–greenstone contacts. In these areas the recrystallized basaltic rock is fine to medium grained, dark grey, and massive to weakly deformed. Deformation intensity of metabasalt is generally low, although narrow (1–20 m-thick) high-strain zones are locally present. Results of five whole-rock analyses of basalts are presented in Appendix 2 (GSWA 156282, 156283, 156284, 156285, 159466).

Metamorphosed medium- to coarse-grained mafic rocks (*Ao*, *Aog*)

Metamorphosed, medium- to coarse-grained mafic rocks (*Ao*, *Aog*) form a small component of the lower greenstone succession on BUNGALBIN. Metagabbros typically form sills and lenses in basaltic rocks (e.g. around MGA 754000E 6626100N and 779600E 6646500N) or are intercalated with

banded iron-formation and chert (e.g. around 749500E 665800N). They are generally conformable with primary igneous layering or bedding and some may represent coarser grained intervals in thick mafic extrusive lavas.

Deeply weathered gabbroic rocks (*Ao*) are typically massive and purplish to reddish-brown with a relict igneous texture. They are distinguished from deeply weathered basalt by a medium to coarse grain size, and from deeply weathered felsic rocks by the lack of primary quartz.

Fresh medium- to coarse-grained metagabbros (mapped as *Aog*) are most abundant in the lower part of the lower greenstone succession, and locally intrude granitoid rocks. Individual gabbro lenses or sills range from 20 to 150 m in thickness, and are typically discontinuous along strike. In thin section these rocks consist of equigranular amphibole (pseudomorphing clinopyroxene), and intergranular plagioclase. Chlorite, epidote, quartz, and opaque minerals including magnetite are accessory minerals.

Metamorphosed felsic volcanic rocks (*Af*)

On BUNGALBIN volcanic and volcanoclastic rocks are most abundant in the Marda Complex (Hallberg et al., 1976; Riganti and Chen, 2002; Chen et al., in press) of the upper greenstone succession. In the lower greenstone succession, rare, thin units of typically weathered and deformed quartz-feldspar-phyric rock may represent felsic volcanic and volcanoclastic rock (*Af*). Although most outcrops are too small to be shown at map scale, one thin unit is intercalated with high-Mg basalt on the northeastern limb of the Bungalbin Syncline (MGA 749000E 665300N) where it conforms with regional trends. The rock is pale grey, and about 3 m thick. Although weathered, it contains quartz and feldspar phenocrysts up to 3 mm long in a fine-grained, quartzofeldspathic groundmass. These rocks could be equivalent to the more widespread, but similarly weathered, felsic rocks in the lower greenstone succession on JACKSON (Riganti and Chen, 2002).

Metamorphosed sedimentary rocks (*As*, *Asq*, *Ass*, *Ac*, *Aci*)

Clastic sedimentary rocks (*As*, *Asq*, *Ass*) in the lower greenstone succession are commonly intercalated with chert and banded iron-formation (*Ac*, *Aci*), but are also abundant among poorly exposed rocks in the Mount Dimer Shear Zone. A broad area of undivided metasedimentary rock has also been mapped west of Mount Dimer.

Undivided metasedimentary rock (*As*) includes shale, siltstone, fine-grained sandstone, and cherty bands. These rocks are typically deeply weathered and poorly exposed. Their sedimentary protolith identification is based on the presence of bedding and the intercalation with chert and banded iron-formation. Quartz grains (1–2 mm in size) are visible in hand specimens of coarser grained sedimentary rocks. Weathered metasedimentary rocks may contain a bedding-parallel foliation (e.g. MGA 747700E 6641600N). These rocks are relatively abundant in the poorly exposed Mount Dimer Shear Zone (Fig. 4), where they are

typically strongly foliated (e.g. MGA 745500E 6665500N). An extensive area of very deeply weathered or altered rocks at the southern end of Hunt Range, west of Mount Dimer, is classified as undivided metasedimentary rock. However, extreme alteration in this area makes it difficult to determine the protolith. Although there are outcrops of deeply weathered shale (e.g. MGA 776300E 6638600N and MGA 777200E 6640300N) and chert (pyritic at MGA 778800E 6638200N), most outcrops consist of very fine grained, bleached saprolite. Well-rounded quartz granules in some saprolite (e.g. MGA 778300E 6638400N) could be interpreted as amygdalites. If this is the case, the unit may include extremely weathered, probably mafic, volcanic rock. Much of the area is covered by abundant scree of vein quartz, giving it a light colour on aerial photos, and a very high reflectance on Landsat images.

Metamorphosed quartz-rich sedimentary rock consisting mainly of quartzite (*Asq*) is white to pale grey and composed predominantly of quartz (>95%), with accessory chlorite, biotite, amphibole, and magnetite. The quartzite is very fine to coarse-grained with fine bedding (down to <1 mm scale) defined by variations in grain size, with thicker beds (up to 20 cm) that locally preserve cross-bedding. It is associated with a major unit of chert and banded iron-formation in the middle association of the lower greenstone succession. In the northern Hunt Range greenstone belt, a quartzite unit (20–30 m thick) is exposed on both limbs of a south-plunging syncline. Although bedding on both limbs dips steeply to the west, cross-bedding in the quartzite indicates younging to the west on the eastern limb (e.g. MGA 775800E 6653300N), and to the east on the western limb (e.g. MGA 775200E 6651800N). In the Helena and Aurora ranges, quartzite lenses (1–10 m thick) in a major chert and banded iron-formation unit have not been mapped separately, due to their thinness and discontinuity along strike. Cross-bedding in the quartzites (e.g. MGA 757300E 6639300N) indicates a consistent younging direction towards the core of the Bungalbin Syncline.

Metamorphosed sandstone and siltstone (*Ass*) of the lower greenstone succession are exposed in the Mount Dimer Shear Zone. Fine- to medium-grained quartzofeldspathic sandstone is intercalated with minor siltstone, shale and, locally, quartzite. Foliation is typically subparallel to bedding and has not transposed it. Although foliated and weathered, primary structures such as graded bedding (e.g. MGA 746600E 6663400N) are better preserved in the sandstone and siltstone unit (*Ass*) than in the deeply weathered clastic sedimentary rocks (*As*).

Banded chert (*Ac*) and banded iron-formation (*Aci*) are widely distributed in all greenstone belts on BUNGALBIN. They are particularly abundant in the middle and upper parts of the lower greenstone succession, and form prominent ridges in the Helena and Aurora ranges, Hunt Range, and Yendilberin Hills. There is considerable variation in the iron-oxide content of these rocks, and the terms ‘banded chert’ and ‘banded iron-formation’ represent end members of a spectrum of compositions.

Both banded chert (*Ac*) and banded iron-formation (*Aci*) are typically laminated and thinly bedded at millimetre to centimetre scales. Locally preserved ripple

marks in chert and banded iron-formation suggest a shallow-water depositional environment (cf. Riganti and Chen, 2002). Metamorphosed banded chert (*Ac*) consists of microcrystalline to recrystallized, fine-grained quartz, and minor iron oxides that form grey, white, and brown bands. Ferruginous chert with a dark-brown to black colour represents the deeply weathered version of banded chert. Banded iron-formation (*Aci*) consists of blue or steel-grey to black magnetite–hematite-rich bands, and red jaspilite bands. Cemented scree on slopes of prominent chert and banded iron-formation ridges contains angular and poorly sorted clasts in a siliceous matrix, and has not been mapped separately.

Upper greenstone succession

In the Marda–Diemals greenstone belt (Fig. 3), the upper greenstone succession comprises the Marda Complex (mainly on JACKSON; Riganti and Chen, 2000) and the Diemals Formation (mainly on JOHNSTON RANGE; Wyche et al., 2000). The eastern part of the Marda Complex is exposed on BUNGALBIN (Fig. 4).

Marda Complex (*Afm*, *Afmr*, *Afms*, *Afmisc*, *Afmss*)

The Marda Complex (Hallberg et al., 1976; Chin and Smith, 1983), with the associated Butcher Bird Monzogranite, occupies a roughly elliptical area of about 600 km² (Fig. 3) on JACKSON (Riganti and Chen, 2000), JOHNSTON RANGE (Wyche et al., 2000), and BUNGALBIN (Chen and Wyche, 2001a). The complex, which is unconformable on the lower greenstone succession, comprises andesitic and rhyolitic lava flows and pyroclastic rocks in the upper part, and clastic and volcanoclastic sedimentary rocks in the lower part (Riganti et al., 2000; Wyche et al., 2001b; Riganti and Chen, 2002; Chen et al., in press).

On BUNGALBIN the Marda Complex is exposed in the core of the Bungalbin Syncline and intruded by the Butcher Bird Monzogranite (Fig. 4). Undivided felsic volcanic and volcanoclastic rocks of the Marda Complex (*Afm*) are typically deeply weathered and partly altered to silcrete or kaolinite. They are white or yellowish-white, fine grained, and generally massive with common primary quartz (1–3 mm long) in a fine-grained groundmass. Felsic volcanic fragments up to 3 cm in size are preserved locally (e.g. MGA 752540E 6644350N).

Relatively fresh felsic volcanic rocks in the Marda Complex (*Afmr*) include rhyolitic lava flows and ignimbrite that are massive to weakly foliated. The rhyolitic lava flows are grey to pale grey, and fine grained to porphyritic, with a local flow banding. Quartz- and plagioclase-phyric rhyolite flows contain phenocrysts up to 5 mm long in an aphyric to fine-grained groundmass. Glass is typically devitrified (e.g. MGA 748700E 6648900N). Unfilled vesicles up to 7 mm long are locally abundant in rhyolitic lava flows (e.g. MGA 752000E 6644900N). Rhyolitic ignimbrite is characterized by welding and rheomorphic flow (e.g. MGA 746300E 6648300N) that indicate subaerial deposition (Hallberg et al., 1976; Riganti et al., 2000). A chemical analysis of rhyolite is given in Appendix 2 (GSWA 159440). Andesitic rocks of the Marda Complex are most abundant on

JACKSON (Riganti and Chen, 2000). On BUNGALBIN minor andesite with amygdalae (3–5 mm long) filled by quartz is intercalated with rhyolite and has not been mapped separately.

Weathered and poorly exposed clastic sedimentary rocks in the Marda Complex (*Afms*) are dominated by siltstone, with subordinate shale, sandstone, and pebbly sandstone in which pebbles, 2–3 cm in size, are composed of chert, banded iron-formation, and vein quartz. They are assigned to the Marda Complex because, although poorly exposed on BUNGALBIN, they are locally intercalated with felsic volcanic components of the Marda Complex on JACKSON (Riganti and Chen, 2002). Primary textures (e.g. bedding) in these rocks are generally preserved, despite weathering and a weakly to moderately developed foliation.

Polymictic conglomerate and pebbly sandstone intercalated with minor sandstone and siltstone in the Marda Complex (*Afmisc*) are typically deeply weathered and poorly exposed. Small outcrops of these rocks are scattered in uncemented chert, banded iron-formation, and lateritic gravels on hill tops and slopes. The conglomerate is typically massive and poorly bedded, whereas the intercalated sandstone and siltstone are generally well bedded, with steep to subvertical bedding (e.g. MGA 741500E 6647800N). Angular to rounded clasts in the conglomerate and pebbly sandstone, up to 30 cm (typically 2–10 cm) in size, are in a silicified or ferruginous lithic and sandy matrix. Although chert and banded iron-formation clasts are the most abundant, there are felsic volcanic (e.g. MGA 752500E 6645100N), granitic (e.g. MGA 749200E 6651700N), and basaltic clasts (e.g. MGA 748900E 6646800N) in places.

Sandstone with subordinate siltstone and pelite in the Marda Complex (*Afmss*) are massive to well bedded. Cross-bedding (e.g. MGA 753400E 6647200N) and graded bedding in fine- to medium-grained quartzofeldspathic sandstone indicate a southwestward-younging direction. Siltstone and pelite are typically ferruginous and have been partly altered to laterite.

Granitoid rocks (*Ag*, *Agf*, *Agm*, *Agmf*, *Agbb*, *Agb*, *Agg*, *Aggs*)

Granitoid rocks occupy about 50% of the BUNGALBIN sheet area (Fig. 4) but are, for the most part, poorly exposed. They are dominated by monzogranite and are mainly between greenstone belts, with a small proportion (e.g. the Butcher Bird Monzogranite) within greenstones. The granite–greenstone contacts are either sheared or intrusive, or both.

Undivided granitoid rocks (*Ag*) include deeply weathered rocks, and inaccessible granite exposures interpreted from aerial photos and Landsat images. Near the southern boundary of BUNGALBIN, widespread, weathered granitoid rocks are white or reddish-white and locally contain less weathered monzogranite. They are medium to coarse grained, and massive to weakly foliated, and typically show a relic granular texture. In some outcrops feldspar is completely weathered and only quartz

remains. Weathered granitoid rocks are commonly capped by silcrete. Strongly foliated, weathered granitoid rocks (*Agf*) are mapped separately (e.g. MGA 764300E 6625300N and MGA 748100E 6664600N).

Monzogranite (*Agm*) and its strongly foliated equivalent (*Agmf*) are the most common granitoid rocks on BUNGALBIN. Monzogranite (*Agm*) is typically massive to weakly deformed, fine to coarse grained, and equigranular to sparsely porphyritic. It is mainly composed of microcline, albitic plagioclase, and quartz, with minor biotite. Microcline phenocrysts are up to 15 mm across, and plagioclase is commonly zoned and sericitized. Biotite, which comprises up to 8% (but is typically less than 5%) of the rock, is the major mafic constituent. Minor hornblende is present locally. Chlorite is a common secondary mineral after biotite, and accessory minerals include opaque oxides (mainly magnetite), apatite, titanite, and zircon.

Well-exposed monzogranite, adjacent to the eastern margin of the northern Hunt Range greenstone belt, is medium to coarse grained, and contains a local foliation that trends north-northwest and dips steeply to the west towards the greenstones. The monzogranite and its contact with greenstones are cut by a set of northeast-trending faults filled by quartz veins. Along the granite–greenstone contact, monzogranite locally contains pegmatite dykes and xenoliths of mafic rocks. The pegmatite dykes are generally parallel to the contact and contain K-feldspar megacrysts up to 10 cm across (e.g. MGA 774000E 6665900N). A sensitive high-resolution ion microprobe (SHRIMP) U–Pb zircon date of 2723 ± 3 Ma has been obtained from recrystallized biotite monzogranite at Kurrajong Rockhole (Nelson, 2002). A geochemical analysis of this sample (GSWA 159422) is presented in Appendix 2.

The Butcher Bird Monzogranite (*Agbb*) is a massive, medium- to coarse-grained, plagioclase-phyric granophyre. It outcrops near the central-western edge of BUNGALBIN (Fig. 4), and extends westwards onto JACKSON (Riganti and Chen, 2000). Petrographically, it is distinguished by prominent plagioclase and, less commonly, K-feldspar megacrysts up to 6 mm long that are commonly sericitized and clouded (Riganti and Chen, 2002). Subordinate quartz phenocrysts are typically resorbed. The Butcher Bird Monzogranite has yielded a SHRIMP U–Pb zircon age of 2730 ± 4 Ma (Nelson, 2001; Riganti and Chen, 2002). The ubiquitous granophyric texture of the monzogranite and the resorbed quartz grains indicate that it represents a high-level intrusion. Its chemical and age similarity to the Marda Complex rhyolite suggests that the monzogranite is coeval with the felsic volcanism (Hallberg et al., 1976; Riganti et al., 2000; Chen et al., in press).

Strongly foliated monzogranite (*Agmf*) is exposed in the Mount Dimer Shear Zone (e.g. MGA 745000E 6671500N), and in areas adjacent to granite–greenstone contacts (e.g. MGA 773700E 6655200N). It is similar to the massive and weakly deformed monzogranite (*Agm*), but contains a pervasive foliation. Within the Mount Dimer Shear Zone, an early, northerly trending foliation is defined by flattened feldspar and quartz grains. The early

foliation is subparallel to a locally developed gneissic banding, and both the early foliation and the gneissic banding are sinistrally displaced by a later, northwest-trending foliation that is defined mainly by preferred alignment of biotite. Some feldspar megacrysts contain brittle fractures perpendicular to the early foliation.

Where granitoid rocks and irregularly interleaved mafic rocks cannot be separated at 1:100 000 scale, they are mapped together as *Agb*. In the northwestern section of the Mount Dimer Shear Zone (e.g. around MGA 747600E 6666600N), strongly foliated to mylonitic monzogranite is interleaved with basaltic and minor pelitic schists, with a pervasive, northwest-trending, steep foliation. In the northern part of the Hunt Range greenstone belt, medium- to coarse-grained massive monzogranite and pegmatite dykes are interleaved with fine-grained, dark-grey to greenish-grey (epidotized) basalt, and minor medium-grained gabbro that are preserved as irregular patches in the monzogranite.

A small pluton of medium-grained, dark-grey granodiorite (*Agg*) outcrops at the southern end of the Mount Manning greenstone belt (MGA 754400E 6675400N). A weak vertical foliation is defined by preferred alignment of mafic minerals and trends 325° , parallel to the granite–greenstone contact. Biotite and minor hornblende comprise up to 10% of the granodiorite. A small body of pink syenite (*AgS*) has intruded strongly foliated granite (*Agf*) in the Mount Dimer Shear Zone (around MGA 748200E 6664800N). The syenite is moderately foliated and contains medium- to coarse-grained K-feldspar phenocrysts (up to 6 mm long) in a fine-grained quartzofeldspathic groundmass, with minor biotite and opaque minerals.

Veins and dykes (*q*, *g*)

Most quartz veins (*q*) on BUNGALBIN trend east and northeast. The most prominent northeast-trending quartz veins are exposed adjacent to the eastern margin of the northern Hunt Range greenstone belt, where massive quartz veins are 3–10 m wide, and form low ridges above granitoid rocks and greenstones (e.g. MGA 775400E 6662100N). Greenstones in the northeastern corner of the sheet area contain both northeast- and east-trending quartz veins.

Granitoid dykes (*g*) of mainly monzogranitic composition within greenstones are common near the eastern granite–greenstone contact in the Hunt Range greenstone belt (e.g. MGA 773700E 6667000N). They are up to 30 m wide and trend north-northwest, parallel to the contact.

Mafic dykes (*Pdy*)

A number of prominent east- and northeast-trending magnetic lineaments that crosscut greenstones and granitoid rocks on BUNGALBIN (Figs 4 and 5) are interpreted as fractures or faults filled by mafic and ultramafic dykes (*Pdy*), which represent the latest Precambrian features in the region. The dykes are all concealed on BUNGALBIN, but are readily identified as

pronounced linear anomalies on aeromagnetic images. Similar magnetic anomalies in the areas to the north (e.g. on EVERETT CREEK; Riganti, 2002) correspond to outcropping mafic dykes. Hallberg (1987) reviewed available data on mafic and ultramafic dykes, and suggested that the dykes were probably emplaced between 2.4 and 2.0 Ga in the central Yilgarn Craton, post-dating cratonization.

Lithostratigraphy of the Marda–Diemals greenstone belt

Only small parts of the Mount Manning and Yerilgee greenstone belts are preserved on BUNGALBIN. The lithostratigraphy of these belts, and of the northern Hunt Range greenstone belt, has not been confidently established, and is briefly described in **Regional geological setting**. The following section deals with the lithostratigraphy of the Marda–Diemals greenstone belt on BUNGALBIN.

Lower greenstone succession

The lithostratigraphy of the lower greenstone succession on BUNGALBIN is constrained by the well-defined Bungalbin Syncline (Fig. 6). Like the JOHNSTON RANGE and JACKSON sheets (Wyche et al., 2001a; Riganti and Chen, 2002), the lower greenstone succession on BUNGALBIN consists of three lithostratigraphic associations: lower, middle, and upper (Fig. 7; Chen et al., in press).

Weathered ultramafic rocks at the base of the lower association are marked by a poorly exposed silica caprock unit that corresponds to a strong magnetic anomaly on aeromagnetic images (Fig. 5). Near the base of the succession, greenstones are extensively intruded by granitoid rocks that are now deeply weathered. The lower association is dominated by tholeiitic basalt (Fig. 7), with subordinate tremolite–chlorite(–talc) schist, peridotite, and gabbro in the lower part, and thin units of banded iron-formation and chert in the upper part.

The middle association consists of a major banded iron-formation and chert unit, up to 800 m thick, that is locally duplicated by reverse faulting (Fig. 6). It forms prominent ridges in the Helena and Aurora ranges, which rise up to 200 m above the surrounding areas. The lower (southern) part of the association is dominated by banded iron-formation, whereas the upper (northern) part is dominated by chert with intercalated quartzite lenses. The steep bedding of the finely laminated banded iron-formation and chert dips mainly to the north and northwest. Cross-bedding in the quartzites indicates a consistent younging direction towards the core of the Bungalbin Syncline (Fig. 6).

The upper association, which contains six lithological units, is truncated by a D₁ thrust fault (Figs 6 and 7). The association is best preserved in a large-scale F₁ anticline within the northeastern limb of the Bungalbin Syncline. The lithological units are:

- tholeiitic basalt with thin units of banded iron-formation, which is poorly exposed in the lower part of the association, below the D₁ thrust fault;

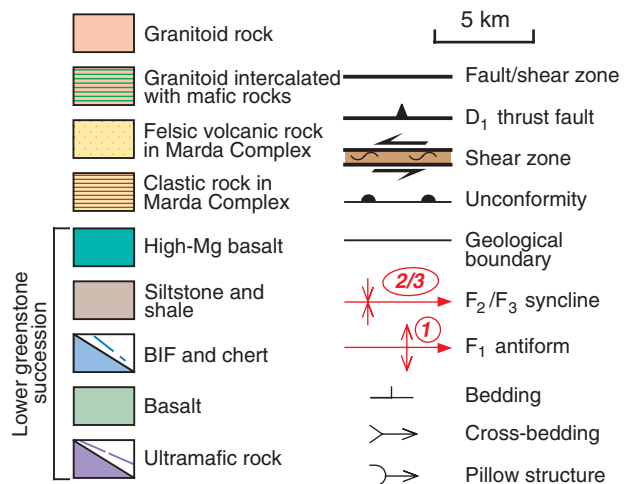
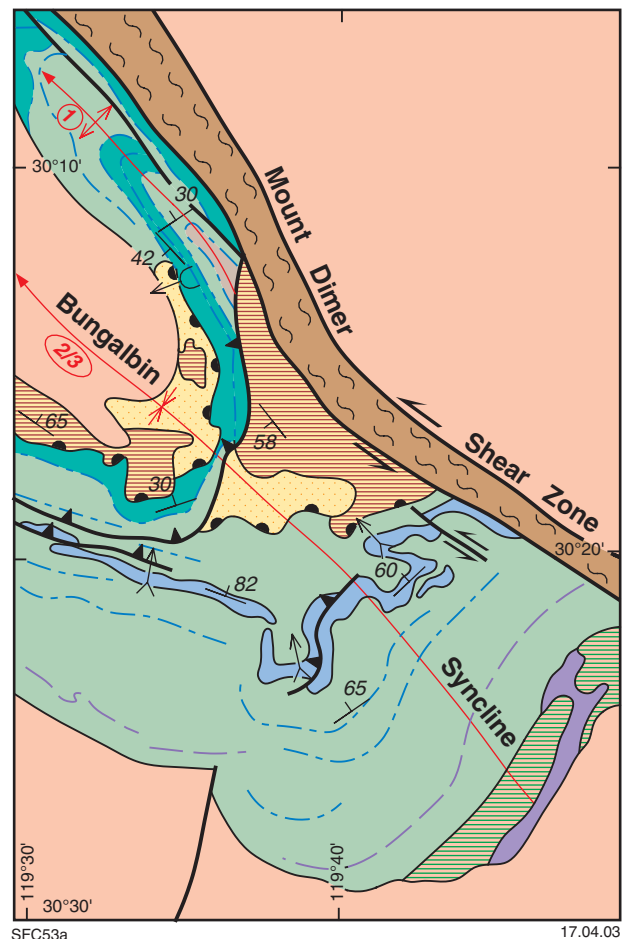


Figure 6. Interpretive geological map of the Marda–Diemals greenstone belt on BUNGALBIN, showing lithostratigraphic distribution and structures

- clastic sedimentary rocks dominated by shale and siltstone in the core of the F₁ anticline that are intercalated with and overlain by banded iron-formation and chert units;
- tholeiitic basalt and minor gabbro intercalated with banded iron-formation and mafic tuff;
- pyroxene-spinifex-textured high-Mg basalt with banded iron-formation intercalations;

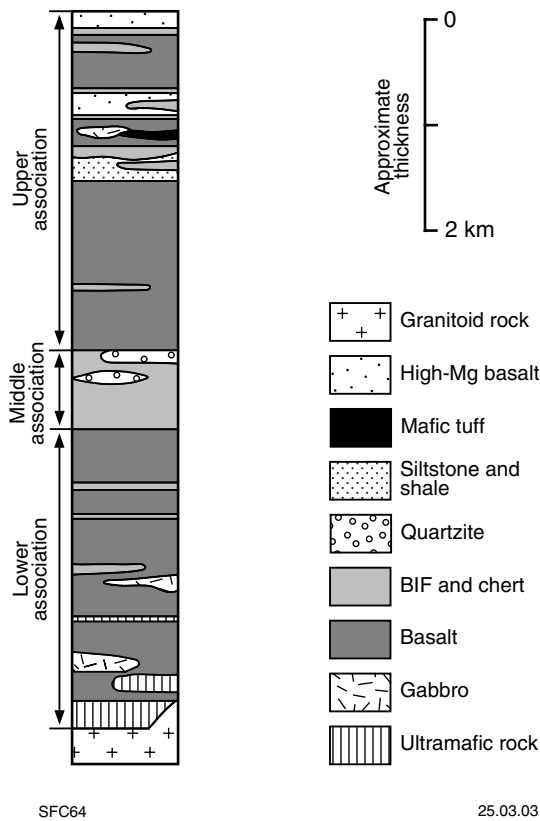


Figure 7. Lithostratigraphic column of the lower greenstone succession on BUNGALBIN

- tholeiitic basalt with thin units of banded iron-formation and chert;
- high-Mg basalt with pyroxene-spinifex texture and pillow-lava structures at the top.

The age of the lower greenstone succession in the Marda–Diemals greenstone belt is poorly constrained. Fletcher et al. (1984) used Sm–Nd model ages to constrain the age of basalt from the Diemals area on JOHNSTON RANGE to 3050 ± 100 Ma. A large body of rhyolitic porphyry at Deception Hill (Fig. 3) within the lower greenstone succession has yielded a SHRIMP U–Pb zircon age of 3023 ± 10 Ma (Nelson, 1999; Wyche et al., 2001a). However, the relationship between this porphyry and adjacent greenstones is concealed, and it is not clear whether it forms part of the succession or represents a later high-level intrusion. It is also possible that the zircons in the porphyry are xenocrysts and that the body is younger than c. 3023 Ma.

The 3 Ga lower greenstone succession in the Marda–Diemals area can be broadly correlated with those in other parts of the Southern Cross Granite–Greenstone Terrane, based on limited geochronological data. For example, Nelson (1995) obtained a SHRIMP U–Pb zircon age of 2958 ± 4 Ma for supracrustal rocks from the Ravensthorpe greenstone belt. In the Lake Johnston greenstone belt, the felsic to intermediate rocks associated with komatiite have given SHRIMP U–Pb zircon ages of 2921 ± 4 and 2903 ± 5 Ma (Wang et al., 1996).

Upper greenstone succession

The upper greenstone succession in the Marda–Diemals greenstone belt consists of felsic to intermediate volcanic and volcanoclastic (Marda Complex) and clastic sedimentary rocks (Diemals Formation) that unconformably overlie the lower greenstone succession (Fig. 3; Chen et al., in press). The Marda Complex (Fig. 8) lies predominantly on JACKSON (Riganti and Chen, 2000, 2002), with a small portion preserved in the western part of BUNGALBIN. The Diemals Formation is absent on BUNGALBIN.

The lower part of the Marda Complex consists of polymictic conglomerate, sandstone, and siltstone that locally interfinger with thin rhyolitic and andesitic units (Fig. 9; Riganti and Chen, 2002; Chen et al., in press). The compositions of conglomerate clasts are similar to adjacent rock types in the lower greenstone succession, with chert and banded iron-formation clasts the most abundant. Locally prominent felsic volcanic clasts are probably derived from contemporaneous felsic volcanic deposits within the complex (Chin and Smith, 1983). The clastic composition and immaturity of the sedimentary rocks suggest proximal deposition (Riganti and Chen, 2002; Chen et al., in press).

The sedimentary rocks in the Marda Complex are conformably overlain by andesite, rhyolite, and subordinate dacite that show a distinct calc-alkaline trend on an AFM plot (Figs 9 and 10; Riganti and Chen, 2002; Chen et al., in press). Dark-grey andesite flows are typically porphyritic and commonly amygdaloidal, and mainly outcrop on JACKSON (Riganti and Chen, 2000, 2002). Rhyolitic ignimbrite and rhyolite flows overlie the andesite and sedimentary rocks (Fig. 9). The rhyolitic rocks preserve evidence of welding and rheomorphic flow that indicate subaerial deposition (Hallberg et al., 1976; Riganti et al., 2000). Two samples taken from rhyolitic ignimbrite on JACKSON yielded SHRIMP U–Pb zircon ages of 2734 ± 3 and 2732 ± 3 Ma respectively (Nelson, 2001; Riganti and Chen, 2002).

Structural geology

The deformation history of the Southern Cross Granite–Greenstone Terrane has been described by Griffin (1990), Bloem et al. (1997), Dalstra et al. (1999), Greenfield and Chen (1999), and Chen et al. (2001, in press). Many authors envisage a north–south compressional regime followed by an east–west compressional regime, although the structural schemes differ in detail. For example, Dalstra et al. (1999) recognized five deformation events between Southern Cross and Diemals:

- north–south D_1 compression produced regional detachment and localized recumbent folds;
- east–west D_2 compression resulted in regional-scale upright to inclined folds;
- further east–west compression during D_3 and D_4 produced regional-scale ductile shear zones and conjugate ductile–brittle faults respectively;
- relaxation and north–south compression (D_5) resulted in localized brittle reactivation and thrusting (Dalstra, 1995; Dalstra et al., 1999).

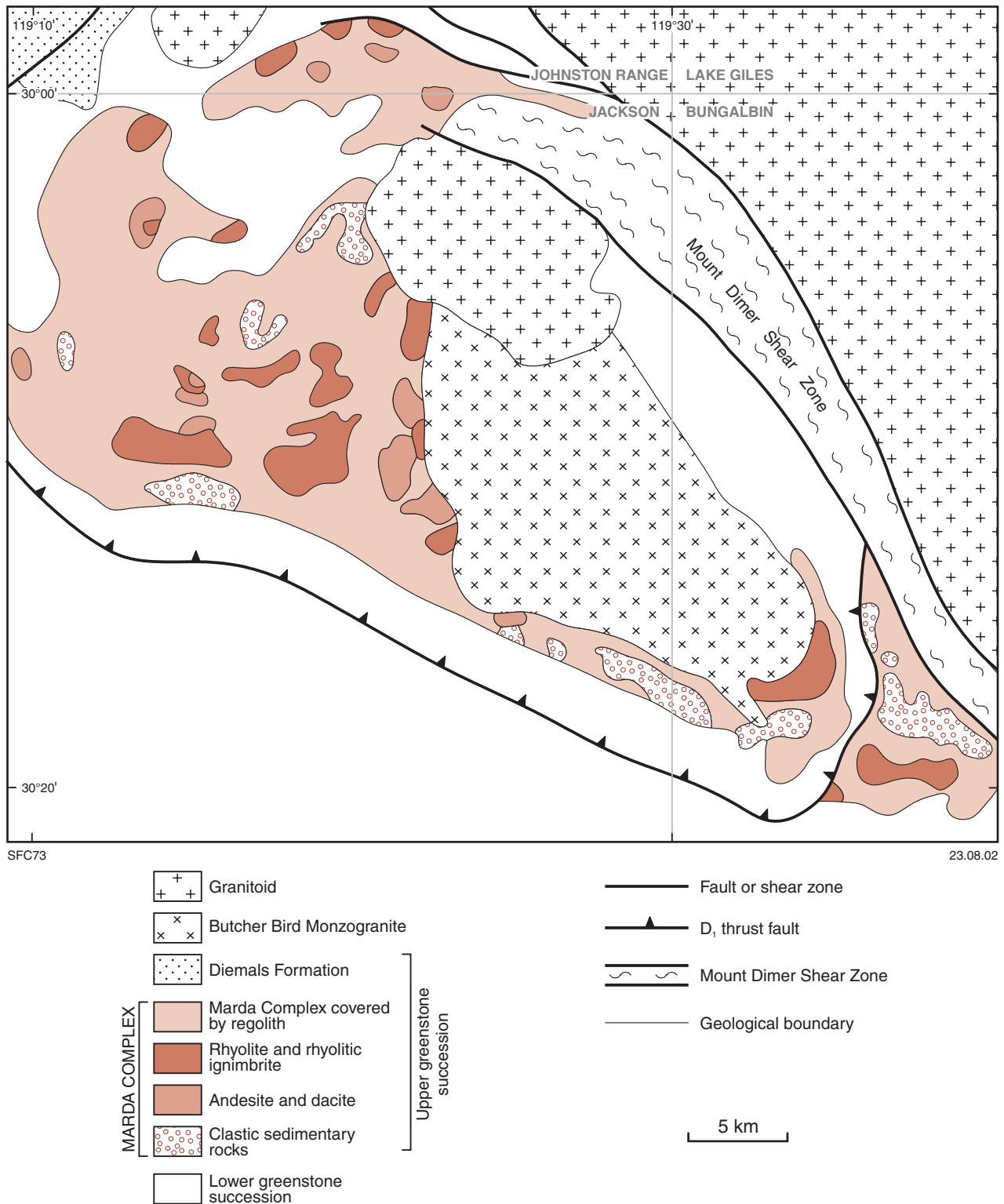


Figure 8. Simplified geological map of the Marda Complex, showing the distribution of major lithological types and the interpreted relationship with the adjacent lower greenstone succession (modified from Riganti and Chen, 2002)

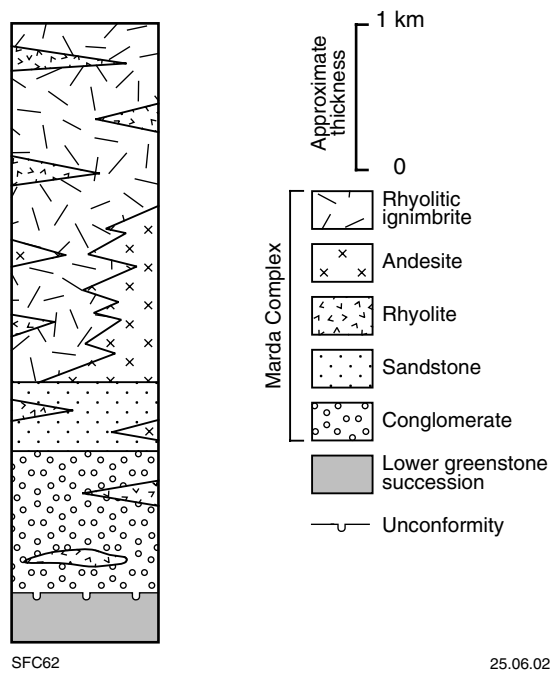


Figure 9. Lithostratigraphic column of the Marda Complex (after Riganti and Chen, 2002)

The previous work and overprinting relationships, deformation styles, and structural orientations have led to the recognition of three principal deformation events in the Marda–Diemals and adjacent areas during recent geological mapping: D_1 , D_2 , and D_3 (Table 1; Chen and Wyche, 2001a; Greenfield, 2001; Wyche et al., 2001a; Riganti and Chen, 2002; Chen et al., in press).

First deformation event (D_1)

Although D_1 structures have been widely observed in the central Southern Cross Granite–Greenstone Terrane (Greenfield and Chen, 1999; Chen et al., in press), evidence for D_1 north–south compression is limited on BUNGALBIN. Figure 6 shows a large-scale D_1 thrust with associated foliation that is generally subparallel to the bedding of shale, siltstone, banded iron-formation, and chert, but locally truncates the axial trace of a large-scale F_1 anticline. The thrust fault extends to the west across the central part of JACKSON (Riganti and Chen, 2000), and is folded around the hinge of the Bungalbin Syncline. The syncline is interpreted as an F_2 fold that has been reoriented during D_3 (Chen et al., 2001; Chen et al., in press). An interpreted D_1 thrust (around MGA 755200E 6637000N) in the Helena and Aurora ranges resulted in stratigraphic duplication of the ridge-forming chert and banded iron-formation unit in the hinge zone of the Bungalbin Syncline (Fig. 6). A large-scale F_1 anticline on the northeastern limb of the Bungalbin Syncline plunges moderately (30° at MGA 748900E 6657800N) to the northwest. Small-scale F_1 tight to isoclinal folds with gently to moderately plunging hinges (e.g. MGA 750400E 6645800N and 759400E 6638300N) are preserved in the hinge zone of, and are overprinted by, the Bungalbin Syncline.

The age of the first deformation event is not well constrained in the central Southern Cross Granite–Greenstone Terrane. However, it post-dated deposition of the lower greenstone succession, as D_1 has clearly affected the middle and upper associations. Lack of D_1 structures in the upper greenstone succession suggests that D_1 deformation ended before c. 2.73 Ga, which is the age of the upper succession.

Second deformation event (D_2)

D_2 east–west compression produced macroscopic upright folds with a weak axial-planar foliation in greenstones, and a northerly trending gneissic banding and foliation in granitoid rocks (Chen et al., in press). The most conspicuous D_2 structure is the Bungalbin Syncline, which has a wavelength of 35 km and straddles the BUNGALBIN and JACKSON sheets. This fold was shown as a syncline by Griffin (1990) and as an anticline by Myers and Swager (1997). The recent mapping confirms it to be a synclinal structure because: (1) field observations and magnetic patterns indicate that the bedding of banded iron-formation and chert units in the hinge zone dips mainly to the northwest towards the core of the fold; (2) cross-bedding in lenticular quartzites and pillow-lava structures in tholeiitic and high-Mg basalts indicate a consistent younging direction towards the core of the fold.

In the northern Hunt Range greenstone belt, a large-scale, north-trending F_2 syncline (Fig. 4) is outlined by a major chert and banded iron-formation unit that is underlain by quartzite and mafic rocks. Bedding on both limbs dips steeply to the west, but cross-bedding in the quartzite indicates younging towards the core of the syncline. A steep to vertical S_2 foliation is weakly

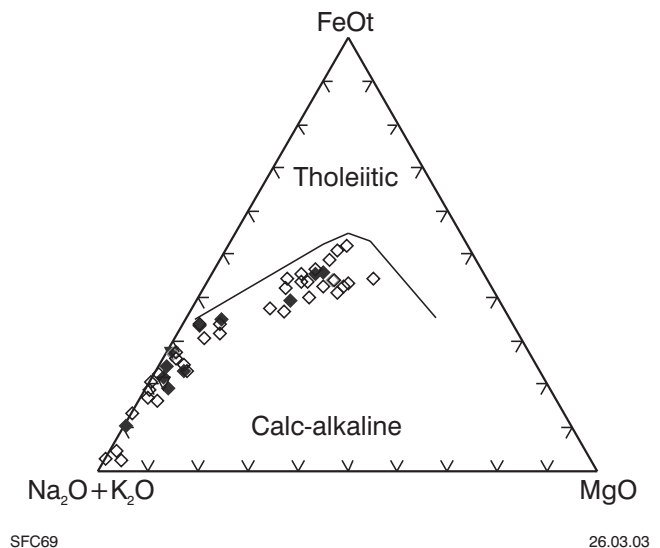


Figure 10. AFM plot indicating the calc-alkaline affinity of the Marda Complex volcanic rocks (after Riganti and Chen, 2002). Filled diamonds are GSWA data, and unfilled diamonds are data from Hallberg et al. (1976). The calc-alkaline–tholeiitic discriminant line is from Irvine and Baragar (1971)

Table 1. Geological evolution of BUNGALBIN and adjacent areas

Age	Deformation event	Geology
3.0 Ga		Deposition of lower greenstone succession
	D ₁	North–south compression: low-angle thrusts, layer-parallel foliation, and tight to isoclinal folds in lower greenstone succession
2.73 Ga		Deposition of Marda Complex felsic to intermediate volcanic rocks Intrusion of Butcher Bird Monzogranite
	D ₂	Early D ₂ east–west compression: upright to inclined folds (e.g. Bungalbin Syncline), and axial-planar foliation Late D ₂ east–west compression: deposition and deformation of Diemals Formation clastic sedimentary rocks
2.72 Ga – 2.68 Ga		Intrusion and deformation of granitoid rocks Peak metamorphism
2.68 Ga – 2.65 Ga	D ₃	Progressive and inhomogeneous east–west shortening: northeast-trending dextral and northwest-trending sinistral shear zones, and arcuate structures
	Post-D ₃	Northeast- and east-trending brittle faults Intrusion of mafic and ultramafic dykes

developed in the Hunt Range greenstone belt. The foliation trends north to north-northwest, subparallel to the axial trace of the F₂ syncline.

In granitoid rocks the most intense D₂ deformation is in regional-scale shear zones or at granite–greenstone contacts (Chen et al., in press). In strongly foliated to gneissic monzogranite within the Mount Dimer Shear Zone (e.g. around MGA 747600E 6666600N and 744800E 6671400N), a northerly trending, steep S₂ foliation is sinistrally truncated by a northwest-trending S₃ foliation. In strongly foliated monzogranite adjacent to the western boundary of the Hunt Range greenstone belt (MGA 773700E 6655200N), a north-trending S₂ foliation defined by the preferred alignment of feldspar and biotite is subvertical or dips steeply to the east. However, monzogranite adjacent to the eastern margin of the Hunt Range greenstone belt is less deformed.

In the central Southern Cross Granite–Greenstone Terrane, the age of D₂ is constrained by the maximum depositional age (2729 ± 9 Ma) of the syn-D₂ Diemals Formation obtained from JOHNSTON RANGE (Nelson, 2001; Wyche et al., 2001a; Chen et al., in press). However, D₂-style deformation may have continued episodically until c. 2680 Ma, coinciding with the major period of granitoid intrusion. Some granitoid plutons contain a northerly trending S₂ foliation (Chen et al., 2001).

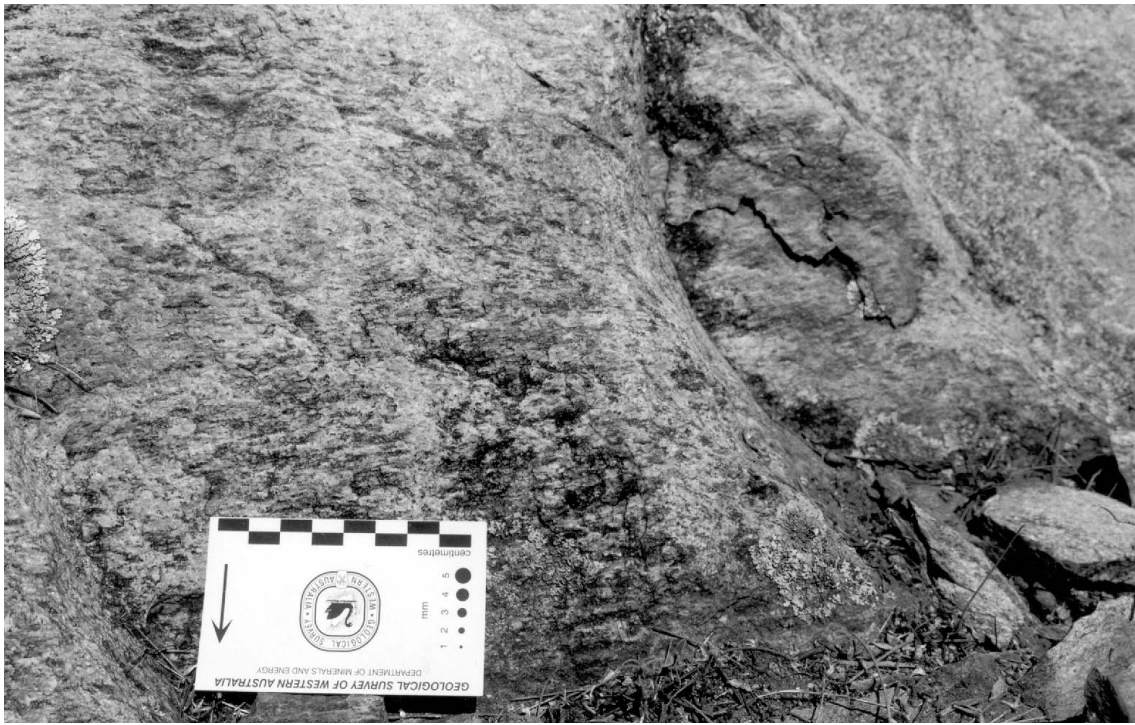
Third deformation event (D₃)

D₃ was a progressive, inhomogeneous east–west shortening event characterized by the development of regional-scale northwest-trending sinistral shear zones and northeast-trending dextral shear zones that are linked by north-trending contractional zones, forming large arcuate structures (Chen et al., 2001). The arcuate structures were generated by the impingement of competent granitoid

blocks into less competent greenstone belts during horizontal shortening (D₃). As a result of granitoid impingement, earlier (F₂) folds were reoriented parallel to the strike-slip shear zones (Chen et al., 2001). According to this model, the northwest-trending Bungalbin Syncline is interpreted as an F₂ fold reoriented during D₃. Both the syncline and Mount Dimer Shear Zone form the south-eastern arm of the Evanston – Mount Dimer arcuate structure (Fig. 3; Chen et al., 2001).

On BUNGALBIN the most prominent D₃ structure is the Mount Dimer Shear Zone, a northwest-trending, regional-scale ductile shear zone, up to 5 km wide. The northwestern section of the shear zone truncates the northeastern limb of the Bungalbin Syncline and juxtaposes it against foliated to gneissic monzogranite. Adjacent to the granite–greenstone contact, granitoid rocks are moderately to strongly foliated and interleaved with mafic and pelitic schists (e.g. MGA 748000E 6664400N and 747300E 6666500N). A steep foliation in granitoid rocks, with a gently plunging mineral lineation (Fig. 11), dips consistently to the northeast, away from the greenstones. The shear zone is centred 1.5 – 2 km in the granitoid rocks, where it is defined by granitic mylonite. The S–C fabrics are well developed in the shear zone centre, where a northerly trending S-plane, defined by the alignment of feldspar, quartz, and biotite, is sinistrally displaced by a northwest-trending C-plane (Fig. 12). Asymmetric porphyroclasts of feldspar (Fig. 12) and small-scale discrete shear zones also indicate a sinistral shear sense.

The Mount Dimer Shear Zone extends to the south-eastern part of BUNGALBIN, where it is poorly exposed but clearly truncates the Hunt Range greenstone belt on aeromagnetic images (Fig. 5). Exploration drillhole data reveal a 2–3 km-wide high-strain zone in which ultramafic and mafic rocks are commonly foliated. Mesoscopic



SFC71

26.06.02

Figure 11. Gently (5°) plunging mineral lineation in strongly foliated monzogranite within the Mount Dimer Shear Zone (MGA 744700E 6671500N)



SFC70

26.06.02

Figure 12. S-C fabrics in strongly foliated monzogranite (MGA 747600E 6666700N), showing sinistral shear sense in the Mount Dimer Shear Zone. Asymmetric feldspar porphyroclasts also indicate sinistral shear sense

S-shaped asymmetric folds in a major chert and banded iron-formation unit (e.g. MGA 783000E 6632400N) and the drag pattern of the Hunt Range greenstone belt indicate a sinistral movement on the shear zone.

Impingement of rigid granitoids into greenstone belts during D_3 has resulted in the lateral escape of greenstone belts (Chen et al., 2001). Adjacent to the southeastern margin of the Marda–Diemals greenstone belt (e.g. MGA 765300E 6627600N), a subvertical to steeply northwesterly dipping foliation in both greenstones and granitoid rocks contains a moderately to steeply plunging mineral lineation. Development of this foliation is attributed to the southeastward escape of the Marda–Diemals greenstone belt during D_3 .

In the central Southern Cross Granite–Greenstone Terrane, strongly foliated monzogranite in the Evanston Shear Zone on LAKE GILES (Greenfield, 2001) has yielded a SHRIMP U–Pb zircon date of 2654 ± 6 Ma (Nelson, 2001). This date is within error of the 2656 ± 3 Ma date obtained by Qiu et al. (1999) for an undeformed porphyritic granitoid intruding the Koolyanobbing Shear Zone near Koolyanobbing, about 40 km south of BUNGALBIN. If strike-slip deformation along the Evanston and Koolyanobbing Shear Zones represents the same event (D_3), then the minimum age for D_3 is c. 2655 Ma.

Post- D_3 deformation

Post- D_3 structures on BUNGALBIN include widespread northeast- and east-trending brittle faults or fractures. Some northeast-trending faults are filled by quartz veins (e.g. MGA 775400E 6662200N), whereas most east-trending faults are probably filled by Proterozoic mafic dykes. These later structures crosscut all the earlier structures, but the timing of deformation is uncertain.

Metamorphism

Binns et al. (1976) published the first regional metamorphic study of the eastern part of the Yilgarn Craton. Ahmat (1986) carried out a more detailed petrographic study of metamorphic assemblages in the Southern Cross Granite–Greenstone Terrane, and refined the map of Binns et al. (1976). A structural and metamorphic study that included the Marda–Diemals region (Dalstra, 1995; Dalstra et al., 1999) included a petrographic study and detailed pressure–temperature determinations on amphibole–plagioclase pairs in metamorphosed tholeiitic mafic rocks from a number of localities west and northwest of BUNGALBIN, and on JACKSON and JOHNSTON RANGE. This study proposed a two-stage metamorphic history.

The first metamorphic episode is best preserved in prehnite–pumpellyite facies rocks, mainly in and around the Marda Complex. Here, much of the primary mineralogy, including igneous clinopyroxene, is retained. The generally very low strain and spilitization of these rocks suggest that they were metamorphosed in a marine basin with a relatively high geothermal gradient and relatively low fluid:rock ratios. Ahmat (1986) attributed the early, very low grade metamorphic event to burial metamorphism.

Subsequent greenschist-facies regional metamorphism affected most greenstones of the lower succession on BUNGALBIN. Dalstra et al. (1999) described low- and high-strain greenschist-facies rocks. Low-strain rocks, particularly finer grained varieties, are commonly altered, but preserve primary igneous features such as porphyritic texture, vesicles, and varioles. Secondary minerals include chlorite, epidote–clinozoisite, albite, and quartz. High-strain rocks are characterized by a strongly developed metamorphic foliation, and igneous features are rarely preserved. In mafic rocks the metamorphic foliation is typically defined by tremolite–actinolite, but also by biotite and chlorite.

Amphibolite-facies rocks are only present at granite–greenstone contacts. Most of the amphibolite-facies rocks mapped on BUNGALBIN are derived from mafic protoliths. They are characterized by dark, blue-green metamorphic hornblende, and may contain clinopyroxene (diopside) and garnet. More-magnesian rocks typically contain tremolite and plagioclase. Banded, diopside- and epidote-bearing amphibolite from the western side of the Yerilgee greenstone belt (MGA 788000E 6670400N) may be derived from calcareous, mafic sedimentary rocks. Dalstra (1995) and Dalstra et al. (1999) showed that although temperatures in amphibolite-facies rocks may have been as high as 540°C , pressures were typically less than 400 MPa. The relatively low pressures involved in the metamorphism of these rocks indicates that the major influence on metamorphic grade was their proximity to the intruding granitoids. Local overprinting of metamorphic minerals by a D_2 – D_3 foliation and the deformation of granitoids in D_3 shear zones suggest that the peak metamorphism was syn- D_2 or earlier. However, the differences in ages of emplacement times of various granitoids implies that attainment of highest metamorphic grades may be diachronous across the region (Wyche et al., 2001a).

The late brittle faults contain retrograde assemblages including chlorite, sericite, and quartz (Dalstra et al., 1999).

Cainozoic geology

More than 75% of BUNGALBIN is covered by regolith, and much of the exposed rock is deeply weathered. Mapping of the regolith combined field observations with interpretation of aerial photos and Landsat images. Some ferruginous, calcareous, and siliceous (silcrete) regolith materials have distinctive colours and patterns on Landsat imagery. The classification system used is that of Hocking et al. (2001), which is based on the RED (Residual–Erosional–Depositional) scheme of Anand et al. (1993).

Relict units (*Rd*, *Rf*, *Rfc*, *Rgp_g*, *Rk*, *Rz*, *Rzu*)

Undivided duricrust (*Rd*) may be either siliceous or ferruginous, and has been mapped predominantly in areas underlain by granitoid rocks. It is typically covered by a thin layer of yellow sand with clay, silt, and nodular and

pisolitic laterite gravel (*Sl*). Lateritic duricrust (*Rf*) is nodular, pisolitic or massive. It is most common over areas of greenstone, particularly in the southwest, and at the southern end of the Hunt Range. Lateritic or ferruginous duricrust commonly forms an apron around ridges of banded iron-formation, but is most widely developed over areas of mafic rock. Lateritic duricrust is locally preserved as ironstone over ridge-forming units (*Rfc*). Although original rock types are unrecognizable, these units were probably metasedimentary rocks (e.g. at MGA 783100E 6636300N a ferruginous ridge caps strongly foliated rock).

Quartzofeldspathic sand over granitoid rock (*Rgp_s*) is characterized by red-yellow sand with sparse, typically weathered granite outcrops. These areas of dominantly residual sand abut, and locally grade into, areas of sandy sheetwash and weathered and fresh granite. Most areas of calcrete (*Rk*) over granites and greenstones are too small to show at map scale. They are commonly associated with drainage. Silcrete or siliceous duricrust (*Rz*) is common over granite, and is best exposed in breakaways. However, most areas of silcrete are too small to be shown at map scale. Silica caprock over ultramafic rock (*Rzu*) is most abundant in areas of deep weathering. On BUNGALBIN silica caprock is locally abundant at the southern end of the Hunt Range, and in the south-central part near the granite–greenstone contact. In the latter area the caprock is the only surface indication of a substantial ultramafic unit that has been extensively intruded by granite. The only other indications of its existence are a prominent magnetic anomaly (Fig. 5) and chips from mineral exploration drillholes (MGA 768400E 6632100N).

Depositional units (*C*, *Cgp_s*, *Clc_i*, *Cf*, *Cq*, *W*, *Wf*, *Wq*, *A*, *A_p*, *L_i*, *L_d*, *L_m*, *S*, *Sl*)

Undivided colluvium (*C*) includes proximal deposits of coarse to fine talus ranging from boulder gravel to silt on steep to gently sloping ground adjacent to greenstone outcrops, breakaways, and on ridge flanks. Colluvium has been further subdivided where clasts and talus are dominated by a particular composition or lithotype. Thus, colluvium adjacent to granitoid outcrops typically comprises quartzofeldspathic material (*Cgp_s*) including granitic scree, silcrete, and quartz-vein pebbles, and quartzofeldspathic sand. Flanks of ridges that are dominated by chert and banded iron-formation scree (*Clc_i*) grade downslope into areas with abundant finer ferruginous colluvium (*Cf*). Colluvium of angular quartz clasts (*Cq*) is common adjacent to prominent quartz veins.

Away from areas of outcrop and colluvium, sheetwash deposits cover very gently sloping plains, typically adjacent to areas of drainage. Undivided sheetwash deposits (*W*) may comprise sand, silt, and clay. However, where the sheetwash is derived from ferruginous source areas, it contains abundant fine, ferruginous grit. Ferruginous sheetwash (*Wf*) can be distinguished by its dark red-brown pattern on aerial photos. An extensive area of sheetwash dominated by quartz-rich debris (*Wq*) lies west of Mount Dimer. The medium to coarse gravel of angular white quartz lies on light-brown silty soil, and it

is commonly associated with leached and bleached, white, very fine grained rock, some of which is clearly metasedimentary (see *As*). Thus the whole area has a light colour on aerial photos, and a high reflectance on Landsat images. Although there are some small outcropping quartz veins nearby, there is no obvious source for the vast amount of quartz scree in the area. This area appears to have undergone an unusual style of alteration and quartz veining.

Alluvium (*A*), typically containing unconsolidated sand, silt, and gravel, is restricted to areas where clear drainage channels can be recognized. Away from the more elevated areas within greenstone belts, alluvium is mapped in broad, slightly depressed, drainage areas. Some drainage systems contain claypans (*A_p*), which fill with water during major rainfall events.

Drainage in the northern half of BUNGALBIN flows north towards the Lake Giles playa-lake system, which lies mainly on LAKE GILES. Lacustrine deposits along the northern edge of BUNGALBIN represent the southern extremity of this system. Lakes (*L_i*) contain silt, mud, and sand deposits, with a veneer of halite or gypsum, or both. Sand dunes adjacent to playa lakes (*L_d*) may contain sand, silt, and evaporitic minerals. They are active systems and are generally not densely vegetated. More stable, and typically more densely vegetated, areas adjacent to lakes contain mixed alluvial, eolian, and lacustrine deposits (*L_m*).

Sandplain deposits (*S*) characterized by yellow sand, with local minor pisolitic laterite, form extensive sheets over areas of granitoid rocks. This material may be residual in part, but probably contains a substantial eolian component. Sandplain and silt with nodular and pisolitic laterite gravel (*Sl*) is mapped over areas of duricrust. These areas have been mainly interpreted from Landsat images where the underlying duricrust has a distinct iron character. The sand is yellow to reddish-yellow and may have both residual and eolian components.

Economic geology

Gold, iron, nickel, and copper have been the major mineral exploration targets on BUNGALBIN. Only gold has been mined. The only documented base metal mineralization in the region is a small copper deposit hosted by a quartz vein in mafic rocks to the west on JACKSON (Marston, 1979; Riganti and Chen, 2002). No volcanic-hosted massive sulfide (VHMS)-style mineralization has been identified in the Marda Complex.

Gold

Gold has been the most widely sought mineral commodity on BUNGALBIN, with all greenstone areas having been explored to some degree. Several small deposits were mined during the 1990s, but there is no record of gold production before this time.

The greatest gold production on BUNGALBIN has come from the Mount Dimer operation of Tectonic Resources NL (Fig. 2). This deposit, described by McIntyre and

Czerw (1998), contains several lode-gold orebodies, and some minor laterite-hosted orebodies. The lode deposits are hosted in both granitic and mafic rocks at the contact between extensive granite, mainly monzogranite, to the south and a greenstone succession containing mafic and ultramafic rocks to the north. The gold is in north-northwesterly striking, east-dipping shear zones. The mineralized shoots are associated with laminated quartz-sulfide veins and, locally, in massive sulfide veins. There are common mafic xenoliths in the granite, and the greenstones are locally metamorphosed to the amphibolite facies. The Mount Dimer deposit produced 3933.47 kg of gold from 780.68 kt of ore (Western Australian Department of Industry and Resources, mines and mineral deposits information database, MINEDEX). Mining commenced in February 1994 and ceased in August 1997. The mine also produced 5881.17 kg of silver (Resource Information Unit, 2001).

The Aurora gold mine (Fig. 2) is a supergene deposit hosted in iron-rich clays and minor quartz (Resource Information Unit, 2001). The deposit produced 176.39 kg of gold from 13.58 kt of ore between 1996 and 2001 (MINEDEX database). Mining activity at Aurora ceased in 2002 (Amalg Resources NL Quarterly Report, June 2002).

A third small deposit at Taipan, about 6 km east of the main Mount Dimer deposits (Fig. 2), is hosted by mafic rocks. This deposit has a recorded production of 265.91 kg gold. In 1994–95, 184.10 kg of gold was produced from 52 kt of ore (MINEDEX database).

Iron

There has been a considerable amount of exploration for iron ore deposits in the Marda–Diemals region. While potentially economic deposits have been identified to the west and northwest on JACKSON (Riganti and Chen, 2002), no such deposits have been found on BUNGALBIN. However, an inferred resource of 65.7 Mt of ore at a grade of 57.9% iron (i.e. 38 Mt contained metal) has been estimated near Bungalbin Hill (MINEDEX database). The deposits have formed by structurally controlled secondary enrichment of banded iron-formation (BHP, 1954–1983).

References

- AHMAT, A. L., 1986, Metamorphic patterns in the greenstone belts of the Southern Cross Province, Western Australia: Western Australia Geological Survey, Report 19, p. 1–21.
- ANAND, R. R., CHURCHWARD, H. M., SMITH, R. E., SMITH, K., GOZZARD, J. R., CRAIG, M. A., and MUNDAY, T. J., 1993, Classification and atlas of regolith-landform mapping units: CSIRO/AMIRA Project P240A, Exploration and Mining Restricted Report 440R (unpublished).
- BARLEY, M. E., and GROVES, D. I., 1990, Deciphering the tectonic evolution of Archaean greenstone belts: the importance of contrasting histories to the distribution of mineralisation in the Yilgarn Craton, Western Australia: *Precambrian Research*, v. 46, p. 3–20.
- BEARD, J. S., 1979, The vegetation of the Jackson area: Vegetation Survey of Western Australia, 1:250 000 Series, Map and Explanatory Memoir, Vegmap Publications, Perth, 27p.
- BEARD, J. S., 1990, Plant life of Western Australia: Kenthurst, N.S.W., Kangaroo Press, 319p.
- BHP, 1954–1983, Koolyanobbing iron ore exploration: Western Australia Geological Survey, Statutory mineral exploration report, Item 7729 (unpublished).
- BIOLOGICAL SURVEYS COMMITTEE, 1985, The biological survey of the Eastern Goldfields of Western Australia. Part 3. Jackson–Kalgoorlie study area: Records of the Western Australian Museum, Supplement no. 23, 168p.
- BINNS, R. A., GUNTHORPE, R. J., and GROVES, D. I., 1976, Metamorphic patterns and development of greenstone belts in the eastern Yilgarn Block, Western Australia, in *The early history of the Earth* edited by B. F. WINDLEY: London, John Wiley and Sons, p. 303–313.
- BLATCHFORD, T., and HONMAN, C. S., 1917, The geology and mineral resources of the Yilgarn Goldfield, Part III — The gold belt north of Southern Cross, including Westonia: Western Australia Geological Survey, Bulletin 71, 321p.
- BLOEM, E. J. M., DALSTRA, H. J., RIDLEY, J. R., and GROVES, D. I., 1997, Granitoid diapirism during protracted tectonism in an Archaean granitoid–greenstone belt, Yilgarn Block, Western Australia: *Precambrian Research*, v. 85, p. 147–171.
- BUREAU OF MINERAL RESOURCES, 1965, Map showing the results of an airborne magnetic and radiometric survey of the Jackson 1:250 000 area, W.A.: Australia Bureau of Mineral Resources, Record 1965/29 (unpublished).
- BYE, S. M., 1968, The acid volcanic rocks of the Marda area, Yilgarn Goldfield, Western Australia: University of Western Australia, Honours thesis (unpublished).
- CHEN, S. F., LIBBY, J. W., GREENFIELD, J. E., WYCHE, S., and RIGANTI, A., 2001, Geometry and kinematics of large arcuate structures formed by impingement of rigid granitoids into greenstone belts during progressive shortening: *Geology*, v. 29, p. 283–286.
- CHEN, S. F., RIGANTI, A., WYCHE, S., GREENFIELD, J. E., and NELSON, D. R., in press, Lithostratigraphy and tectonic evolution of contrasting greenstone successions in the central Yilgarn Craton, Western Australia: *Precambrian Research*.
- CHEN, S. F., and WYCHE, S., 2001a, Bungalbin, W.A. Sheet 2837: Western Australia Geological Survey, 1:100 000 Geological Series.
- CHEN, S. F., and WYCHE, S., (compilers), 2001b, Archaean granite–greenstones of the central Yilgarn Craton, Western Australia — a field guide: Western Australia Geological Survey, Record 2001/14, 76p.
- CHIN, R. J., and SMITH, R. A., 1983, Jackson, W.A.: Western Australia Geological Survey, 1:250 000 Geological Series Explanatory Notes, 30p.
- DALSTRA, H. J., 1995, Metamorphic and structural evolution of the greenstone belts of the Southern Cross – Diemals region of the Yilgarn Block, Western Australia, and its relationship to the gold mineralization: University of Western Australia, PhD thesis (unpublished).
- DALSTRA, H. J., BLOEM, E. J. M., RIDLEY, J. R., and GROVES, D. I., 1998, Diapirism synchronous with regional deformation and gold mineralization, a new concept for granitoid emplacement in the Southern Cross Province, Western Australia: *Geologie en Mijnbouw*, v. 76, p. 321–338.
- DALSTRA, H. J., RIDLEY, J. R., BLOEM, E. J. M., and GROVES, D. I., 1999, Metamorphic evolution of the central Southern Cross Province, Yilgarn Craton, Western Australia: *Australian Journal of Earth Sciences*, v. 46, p. 765–784.
- DONALDSON, C. H., 1982, Spinifex-textured komatiites: a review of textures, compositions and layering, in *Komatiites* edited by N. T. ARNDT and E. G. NISBET: London, George Allen and Unwin, p. 213–244.
- FLETCHER, I. R., ROSMAN, K. J. R., WILLIAMS, I. R., HICKMAN, A. H., and BAXTER, J. L., 1984, Sm–Nd geochronology of greenstone belts in the Yilgarn Block, Western Australia: *Precambrian Research*, v. 26, p. 333–361.
- GEE, R. D., BAXTER, J. L., WILDE, S. A., and WILLIAMS, I. R., 1981, Crustal development in the Yilgarn Block, in *Archaean Geology* edited by J. E. GLOVER and D. I. GROVES: 2nd International Archaean Symposium, Perth, W.A., 1980, Proceedings; Western Australia Geological Society of Australia, Special Publication, no. 7, p. 43–56.
- GREENFIELD, J. E., 2001, Geology of the Lake Giles 1:100 000 sheet: Western Australia Geological Survey, 1:100 000 Geological Series Explanatory Notes, 19p.
- GREENFIELD, J. E., and CHEN, S. F., 1999, Structural evolution of the Marda–Diemals area, Southern Cross Province: Western Australia Geological Survey, Annual Review 1998–99, p. 68–73.
- GREENFIELD, J. E., CHEN, S. F., WYCHE, S., RIGANTI, A., and NELSON, D. R., 2000, Relative age of felsic magmatism and deformation in the central and eastern Yilgarn Craton, Western Australia, in *Understanding planet Earth, searching for a sustainable future* edited by C. G. SKILBECK and T. C. T. HUBBLE: Geological Society of Australia; 15th Australian Geological Convention, Sydney, N.S.W., 2000; Abstracts, no. 59, p. 191.
- GRIFFIN, T. J., 1990, Southern Cross Province, in *Geology and mineral resources of Western Australia*: Western Australia Geological Survey, Memoir 3, p. 60–77.

- HALLBERG, J. A., 1987, Postorotization mafic and ultramafic dykes of the Yilgarn Block: *Australian Journal of Earth Sciences*, v. 34, p. 135–149.
- HALLBERG, J. A., JOHNSTON, C., and BYE, S. M., 1976, The Archaean Marda igneous complex, Western Australia: *Precambrian Research*, v. 3, p. 111–136.
- HOCKING, R. M., LANGFORD, R. L., THORNE, A. M., SANDERS, A. J., MORRIS, P. A., STRONG, C. A., and GOZZARD, J. R., 2001, A classification system for regolith in Western Australia: *Western Australia Geological Survey, Record 2001/4*, 22p.
- IRVINE, T. N., and BARAGAR, W. R., 1971, A guide to the chemical classification of the common igneous rocks: *Canadian Journal of Earth Sciences*, v. 8, p. 523–548.
- MACKEY, T. E., 1999, Jackson, W.A., *Interpreted geology (1:250 000 scale map)*. Australian Geological Survey Organisation, Canberra.
- MARSTON, R. J., 1979, Copper mineralization in Western Australia: *Western Australia Geological Survey, Mineral Resources Bulletin 13*, 208p.
- MATHESON, R. S., and MILES, K. R., 1947, The mining groups of the Yilgarn Goldfield north of the Great Eastern Railway: *Western Australia Geological Survey, Bulletin 101*, 242p.
- McINTYRE, J. R., and CZERW, A., 1998, Mount Dimer gold deposits *in Geology of Australian and Papua New Guinean mineral deposits edited by D. A. BERKMAN and D. H. MCKENZIE*: The Australasian Institute of Mining and Metallurgy, Monograph 22, p. 191–195.
- MYERS, J. S., 1997, Preface: *Archaean geology of the Eastern Goldfields of Western Australia — regional overview*: *Precambrian Research*, v. 83, p. 1–10.
- MYERS, J. S., and SWAGER, C., 1997, The Yilgarn Craton, *in Greenstone belts edited by M. de WIT and L. D. ASHWAL*: Oxford University Monographs on Geology and Geophysics, Monograph 35, p. 640–656.
- NELSON, D. R., 1995, Compilation of SHRIMP U–Pb zircon dates, 1994: *Western Australia Geological Survey, Record 1995/3*, 244p.
- NELSON, D. R., 1999, Compilation of geochronology data, 1998: *Western Australia Geological Survey, Record 1999/2*, 222p.
- NELSON, D. R., 2001, Compilation of geochronology data, 2000: *Western Australia Geological Survey, Record 2001/2*, 205p.
- NELSON, D. R., 2002, Compilation of geochronology data, 2001: *Western Australia Geological Survey, Record 2002/2*, 282p.
- PIDGEON, R. T., and HALLBERG, J. A., 2000, Age relationships in supracrustal sequences in the northern part of the Murchison Terrane, Archaean Yilgarn Craton, Western Australia: a combined field and zircon U–Pb study: *Australian Journal of Earth Sciences*, v. 47, p. 153–165.
- QIU, Y. M., McNAUGHTON, N. J., GROVES, D. I., and DALSTRA, H. J., 1999, Ages of internal granitoids in the Southern Cross region, Yilgarn Craton, Western Australia, and their crustal evolution and tectonic implications: *Australian Journal of Earth Sciences*, v. 46, p. 971–981.
- RESOURCE INFORMATION UNIT, 2001, Register of Australian Mining 2001/02: Perth, Western Australia, 686p.
- RIGANTI, A., 2002, Everett Creek, W.A. Sheet 2841: *Western Australia Geological Survey, 1:100 000 Geological Series*.
- RIGANTI, A., and CHEN, S.F., 2000, Jackson, W.A. Sheet 2737: *Western Australia Geological Survey, 1:100 000 Geological Series*.
- RIGANTI, A., and CHEN, S.F., 2002, Geology of the Jackson 1:100 000 sheet: *Western Australia Geological Survey, 1:100 000 Geological Series Explanatory Notes*, 51p.
- RIGANTI, A., CHEN, S. F., WYCHE, S., and GREENFIELD, J. E., 2000, Late Archaean volcanism and sedimentation in the central Yilgarn Craton, *in GSWA 2000 Extended abstracts*: *Western Australia Geological Survey, Record 2000/8*, p. 4–6.
- SPENCE, A. G., 1958, Preliminary report on airborne magnetic and radiometric surveys in Kalgoorlie–Southern Cross region, Western Australia (1956–1957): *Australia Bureau of Mineral Resources, Record 1958/45* (unpublished).
- TAYLOR, S. R., and HALLBERG, J. A., 1977, Rare-earth elements in the Marda calc-alkaline suite: an Archaean geochemical analogue of Andean-type volcanism: *Geochimica et Cosmochimica Acta*, v. 41, p. 1125–1129.
- TYLER, I. M., and HOCKING, R. M., 2001, Tectonic units of Western Australia (scale 1:2 500 000): *Western Australia Geological Survey*.
- WALKER, I. W., and BLIGHT, D. F., 1983, Barlee, W.A.: *Western Australia Geological Survey 1:250 000 Geological Series Explanatory Notes*, 22p.
- WANG, Q., SCHIØTTE, L., and CAMPBELL, I. H., 1996, Geochronological constraints on the age of komatiites and nickel mineralization in the Lake Johnston greenstone belt, Yilgarn Craton, Western Australia: *Australian Journal of Earth Sciences*, v. 43, p. 381–385.
- WATKINS, K. P., and HICKMAN, A. H., 1990, Geological evolution and mineralization of the Murchison Province Western Australia: *Western Australia Geological Survey, Bulletin 137*, 267p.
- WOODWARD, H. P., 1912, A general description of the northern portion of the Yilgarn Goldfield and the southern portion of the North Coolgardie Goldfield: *Western Australia Geological Survey, Bulletin 46*, 23p.
- WYCHE, S., CHEN, S. F., GREENFIELD, J. E., and RIGANTI, A., 2000, Johnston Range, W.A. Sheet 2738: *Western Australia Geological Survey, 1:100 000 Geological Series*.
- WYCHE, S., CHEN, S. F., GREENFIELD, J. E., and RIGANTI, A., 2001a, Geology of the Johnston Range 1:100 000 sheet: *Western Australia Geological Survey, 1:100 000 Geological Series Explanatory Notes*, 31p.
- WYCHE, S., CHEN, S. F., GREENFIELD, J. E., and RIGANTI, A., 2001b, Geology and tectonic evolution of the central Yilgarn Craton, Western Australia, *in 4th International Archaean Symposium — extended abstracts edited by K. F. CASSIDY, J. M. DUNPHY, and M. J. VAN KRANENDONK*: *AGSO – Geoscience Australia, Record 2001/37*, p. 109–111.

Appendix 1
**Gazetteer of localities mentioned
in the text**

<i>Locality</i>	<i>MGA coordinates</i>	
	<i>Easting</i>	<i>Northing</i>
Aurora mine	753400	6629950
Bungalbin Hill	753100	6634900
Dooling Soak	755800	6675000
Kurrajong Rockhole	777750	6657750
Mount Dimer	780800	6639100
Mount Dimer mine	771800	6634000
Taipan mine	778200	6634300

Appendix 2

Whole-rock geochemical data for BUNGALBIN

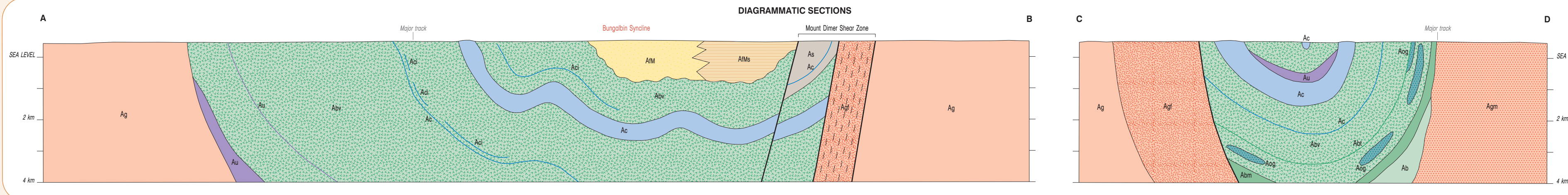
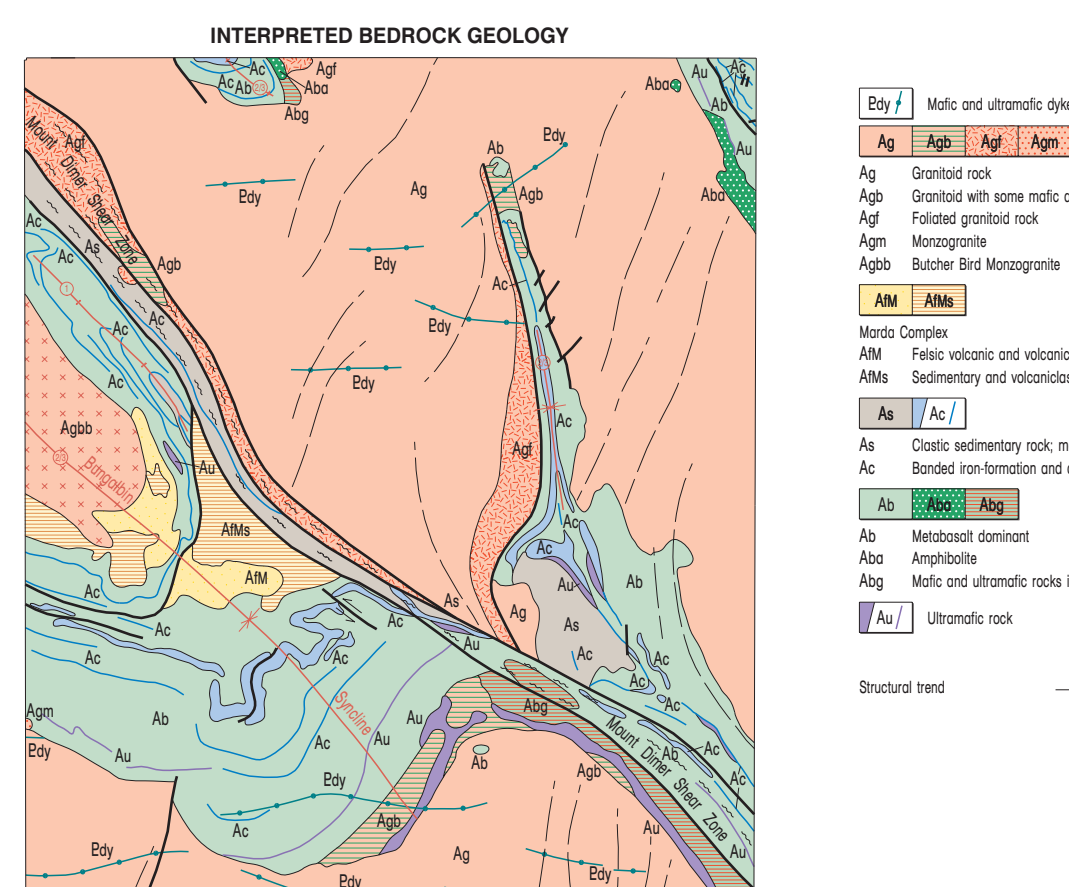
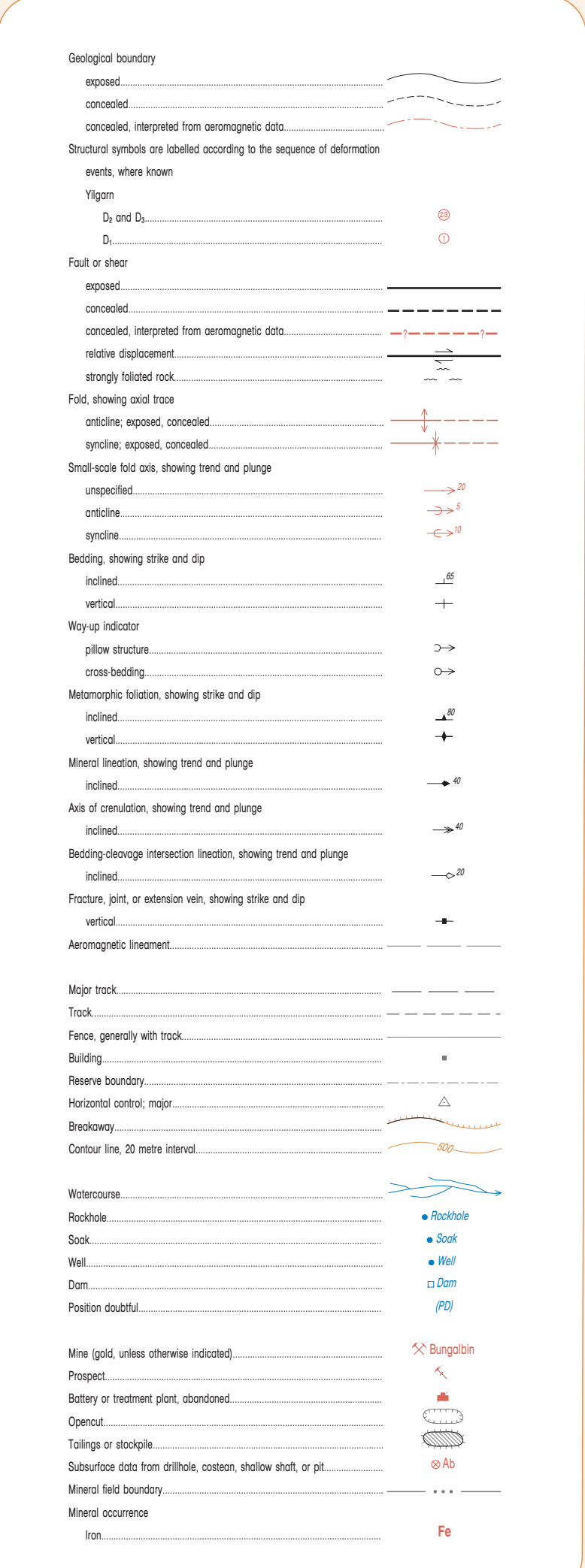
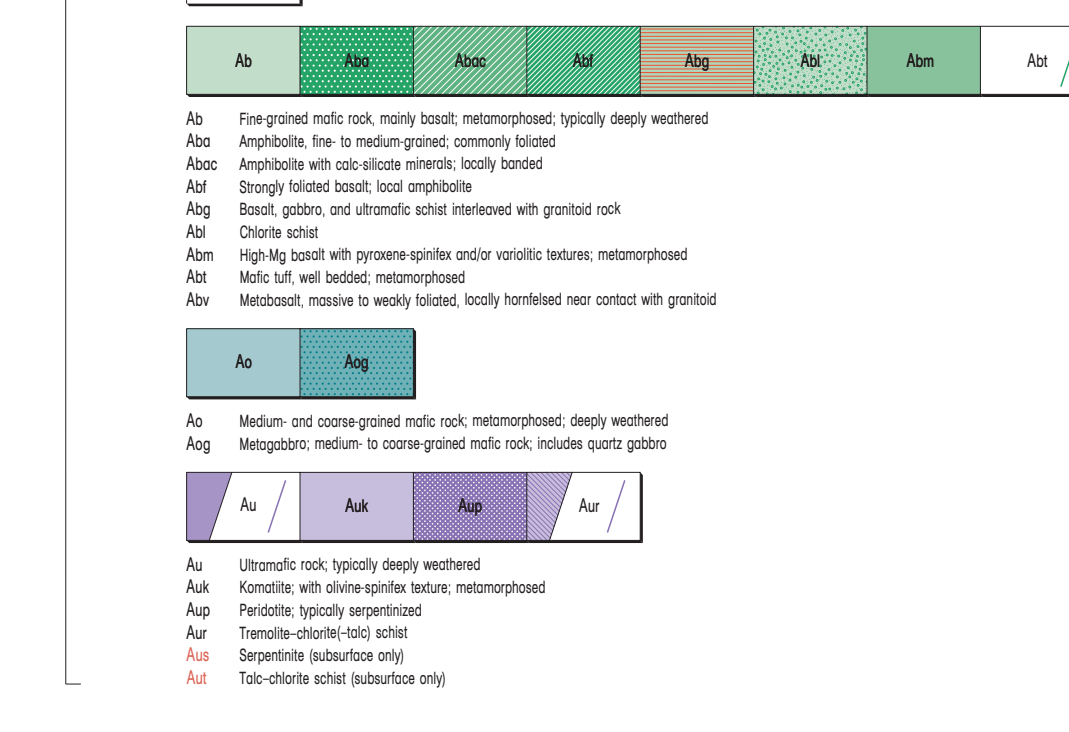
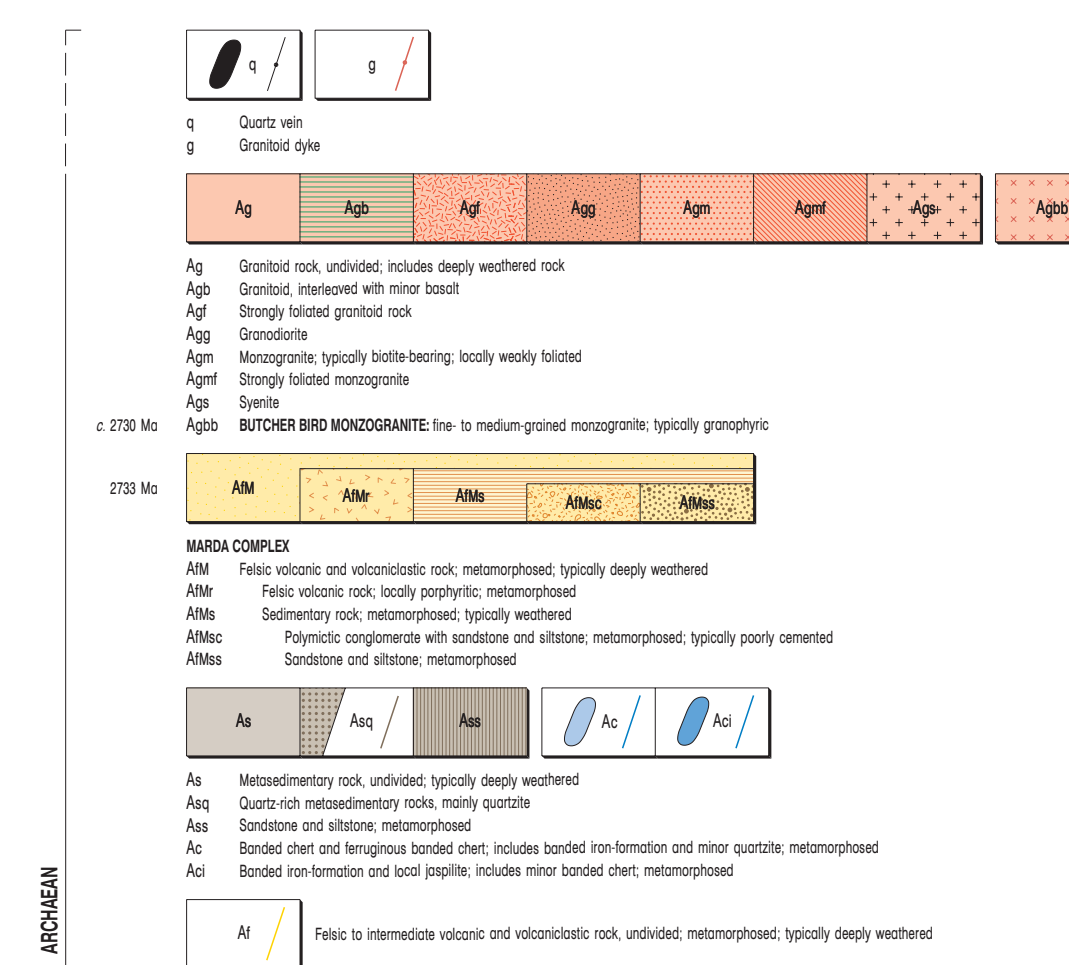
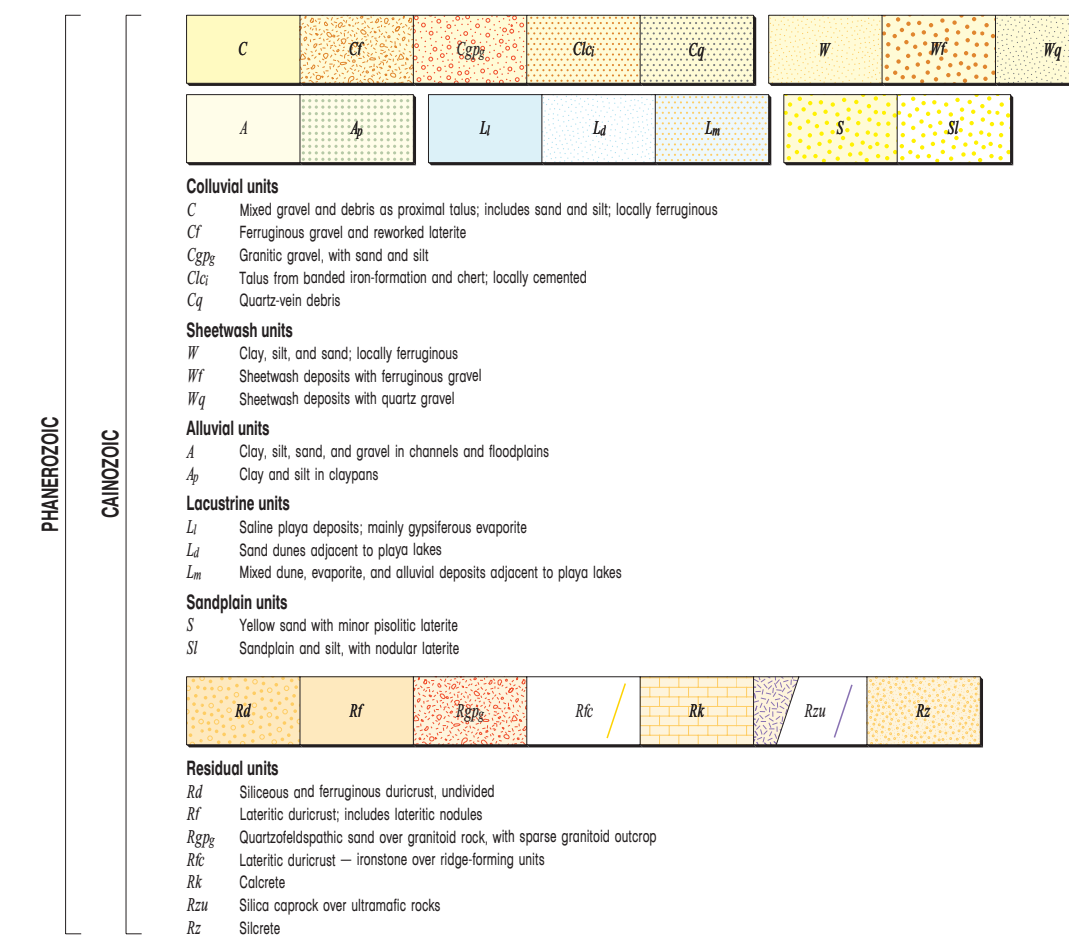
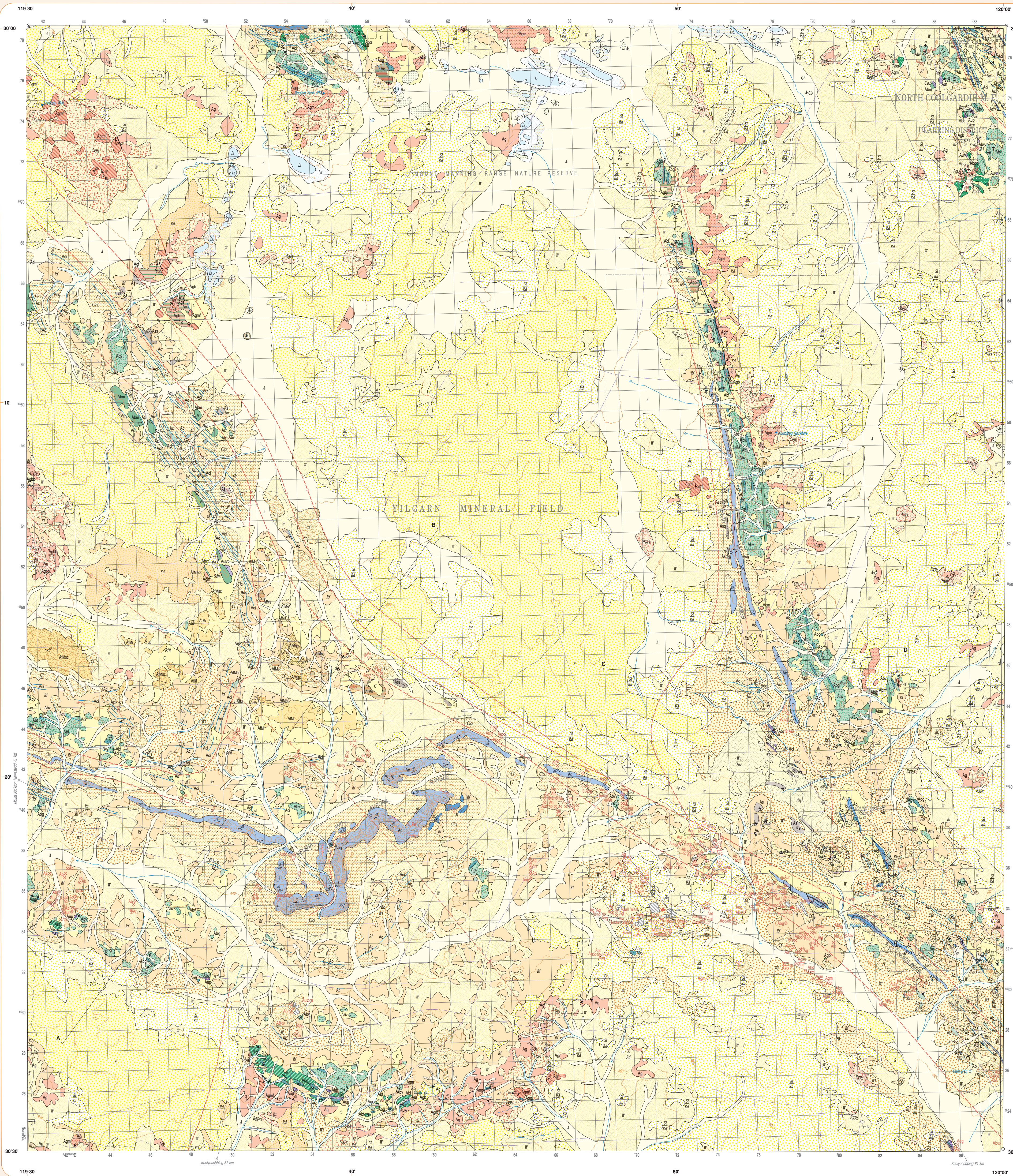
GSWA No.	143363	156282	156283	156284	156285	159416	159422	159432	159440	159442	159466
Rock type	Peridotite	Basalt	Basalt	Basalt	Basalt	Monzogranite	Monzogranite	Granite	Rhyolite	Peridotite	Basalt
Locality	Bungalbin Hill west	Mount Dimer east	Yendilberin Hills	Yendilberin Hills	Yerilgee belt	Hunt Range southeast	Kurrajong Rockhole	Dooling Soak	Bungalbin Hill north	Aurora south	Hunt Range
Easting	742500	784000	784800	781800	787100	778000	777600	754900	748700	755000	776600
Northing	6634600	6639400	6631800	6632100	6675700	6652000	6657900	6674800	6648900	6625900	6652000
	Percentage										
SiO ₂	40.72	50.53	53.66	49.79	52.43	74.39	74.20	74.60	77.26	43.66	54.68
TiO ₂	0.17	0.81	0.62	1.12	0.99	0.25	0.20	0.14	0.30	0.22	0.63
Al ₂ O ₃	3.47	13.88	14.27	14.43	13.13	13.31	13.43	13.55	13.00	4.54	14.43
Fe ₂ O ₃	6.95	1.95	1.49	3.92	2.47	1.03	0.57	0.46	0.45	3.61	2.16
FeO	4.44	8.92	8.23	9.09	9.95	0.95	1.42	1.11	0.41	5.47	6.76
MnO	0.14	0.21	0.16	0.21	0.19	0.04	0.05	0.05	0.01	0.12	0.21
MgO	31.93	7.69	8.27	6.96	6.69	0.30	0.42	0.30	0.06	29.17	5.16
CaO	0.47	11.67	7.96	8.90	9.08	1.04	1.58	1.15	0.16	4.10	14.61
Na ₂ O	<0.02	2.28	2.25	3.45	3.21	3.67	3.77	3.62	4.90	0.00	0.55
K ₂ O	0.01	0.15	0.18	0.33	0.29	4.63	3.91	4.64	2.65	0.01	0.03
P ₂ O ₅	0.01	0.03	0.06	0.08	0.06	0.07	0.04	0.04	0.01	0.01	0.04
BaO	0.00	0.00	0.01	0.01	0.01	0.09	0.08	0.09	0.12	0.01	0.01
S	0.01	0.00	0.00	0.00	0.01	0.00	0.00	0.00	0.03	0.01	0.01
CO ₂	0.11	0.03	0.03	0.04	0.03	0.03	0.01	0.02	0.12	0.03	0.03
H ₂ O-	0.32	0.06	0.05	0.10	0.16	0.09	0.06	0.09	0.23	0.33	0.08
H ₂ O+	10.55	1.24	2.82	1.73	1.42	0.30	0.35	0.36	0.82	8.44	0.82
Total	99.27	99.46	100.06	100.15	100.11	100.18	100.08	100.22	100.52	99.73	100.18
Fe ₂ O ₃ (Total)	11.88	11.86	10.64	14.02	13.53	2.09	2.14	1.69	0.91	9.69	9.67
	Part per million										
Sc	20	48	52	50	47	4.5	4.3	4.1	11	25	45
V	69	259	227	312	272	12	13	8.9	3.9	101	223
Cr	3 415	260	80	180	205	3.9	7.6	4.6	3.1	2 789	410
Ni	1 410	136	70	129	133	2.1	4.7	2.7	5.8	1 610	153
Cu	5.9	40	79	177	76	4.5	8.4	5.7	6.5	35	11
Zn	47	97	58	78	74	32	36	28	9.1	49	65
Ga	3.0	13	14	18	15	15	16	17	16	4.5	16
Ge	0.9	2.5	1.3	1.5	1.2	1.2	1.1	1.4	0.7	0.9	1.3
As	6.7	<0.5	<0.5	<0.5	<0.5	<0.5	<0.5	<0.5	<0.5	<0.5	<0.5
Se	<0.5	<0.5	<0.5	<0.5	<0.5	<0.5	<0.5	<0.5	<0.5	<0.5	<0.5
Br	0.6	<0.5	<0.5	<0.5	<0.5	<0.5	<0.5	<0.5	2.0	<0.5	<0.5
Rb	1.4	2.8	7.4	9.4	9.2	247	210	260	63	1.2	1.0
Sr	3.5	113	94	111	62	127	127	104	74	4.4	90
Y	3.5	18	20	24	21	15	20	14	32	5.1	16
Zr	12	40	40	59	54	154	125	121	367	12	43

Nb	1.4	3.3	2.7	3.7	3.2	14	12	13	14	1.3	3.3
Mo	0.6	0.6	<0.5	<0.5	<0.5	1.7	<0.5	<0.5	1.4	<0.5	<0.5
Ag	0.5	<0.2	<0.2	<0.2	<0.2	<0.2	<0.2	<0.2	<0.2	<0.2	<0.2
Cd	0.4	<0.2	0.2	<0.2	0.2	0.2	<0.2	0.1	<0.2	0.2	0.2
In	<0.2	<0.2	<0.2	<0.2	<0.2	<0.2	<0.2	<0.2	<0.2	<0.2	<0.2
Sn	0.2	0.6	0.2	0.6	0.6	2.9	2.5	2.4	2.5	0.2	0.6
Sb	0.9	0.2	0.3	0.8	0.3	<0.5	<0.5	<0.5	0.5	0.3	0.2
Te	<0.5	<0.5	<0.5	<0.5	<0.5	<0.5	<0.5	<0.5	1.0	<0.5	<0.5
I	<0.7	<0.7	<0.7	<0.7	<0.7	<0.7	<0.7	<0.7	<0.7	<0.7	<0.7
Cs	1.0	1.4	0.7	0.6	1.1	6.4	1.4	3.1	1.4	<0.4	<0.4
Ba	3.8	22	49	91	71	741	620	705	1 012	45	25
La	1.9	2.2	1.6	<1	<1	25	29	35	16	<1	3.6
Ce	2.4	2.7	4.2	1.7	3.0	85	60	64	27	1.1	7.4
Nd	2.7	5.3	2.9	5.7	3.3	17	21	17	10	1.8	6.2
Hf	<3	<3	<3	<3	<3	5.5	3.9	5.3	8.8	<3	<3
Ta	<8	<8	<8	<8	<8	<8	<8	<8	<8	<8	<8
W	<5	<5	<5	<5	<5	<5	<5	<5	<5	<5	<5
Tl	<0.7	<0.7	<0.7	<0.7	<0.7	1.1	0.8	0.8	<0.7	<0.7	<0.7
Pb	2.2	7.5	2.1	6.2	2.0	43	43	53	17	1.8	2.5
Bi	<0.6	<0.6	<0.6	<0.6	<0.6	<0.6	<0.6	<0.6	<0.6	<0.6	<0.6
Th	1.1	<1	<1	<1	<1	38	33	39	24	<1	<1
U	<1	<1	<1	<1	<1	3.8	16.8	6.1	3.6	<1	<1
La	1.527	0.914	–	–	1.531	–	–	–	–	0.425	4.278
Ce	2.643	2.397	–	–	3.670	–	–	–	–	1.234	9.593
Pr	0.395	0.431	–	–	0.750	–	–	–	–	0.211	1.345
Nd	1.631	2.282	–	–	4.153	–	–	–	–	1.090	5.854
Sm	0.450	0.952	–	–	1.770	–	–	–	–	0.396	1.684
Eu	0.148	0.390	–	–	0.701	–	–	–	–	0.065	0.626
Gd	0.538	1.508	–	–	2.607	–	–	–	–	0.556	2.034
Tb	0.094	0.312	–	–	0.482	–	–	–	–	0.103	0.348
Dy	0.624	2.411	–	–	3.353	–	–	–	–	0.737	2.410
Ho	0.134	0.567	–	–	0.729	–	–	–	–	0.169	0.520
Er	0.381	1.801	–	–	2.196	–	–	–	–	0.509	1.504
Tm	0.059	0.286	–	–	0.338	–	–	–	–	0.082	0.232
Yb	0.374	1.822	–	–	2.139	–	–	–	–	0.522	1.495
Lu	0.058	0.296	–	–	0.339	–	–	–	–	0.081	0.232
Σ _{REE}	9.06	16.37	–	–	24.76	–	–	–	–	6.18	32.16
(La/Yb) _{CN}	2.93	0.36	–	–	0.51	–	–	–	–	0.58	2.05

NOTES: Major- and trace-element analyses, including La, Ce, and Nd, were carried out at the Australian National University, Canberra, by X-ray fluorescence (XRF). Complete rare earth element analyses were carried out at the University of Queensland by inductively coupled plasma mass spectrometry (ICP-MS). The techniques are discussed in Morris (2000)

Reference

MORRIS, P. A., 2000, Composition of Geological Survey of Western Australia geochemical reference materials: Western Australia Geological Survey, Record 2000/11, 33p.



Geology by S. F. Chen and S. Wyche 1998-1999
Geoscientist by S. R. Nelson, in press, SGMR Record 280/2
Edited by M. Telford and G. Luan
Cartography by G. Fletcher, P. Taylor, and B. Williams
Copyright from the Department of Land Administration Sheet 89-12, 2837, with modifications from geological field survey
Published by the Geological Survey of Western Australia. Copies available from the Information Centre, Department of Mines and Energy, 100 Plain Street, East Perth, WA, 6004. Phone 08 9221 3465 Fax 08 9221 2444
This map is also available in digital form
Printed by Frank Daniels Pty Ltd, Western Australia
The recommended reference for this map is:
Chen, S. F. and Wyche, S., 1999, Bungalbin, W.A. Sheet 2837, Western Australia Geological Survey, 1:100 000 Geological Series